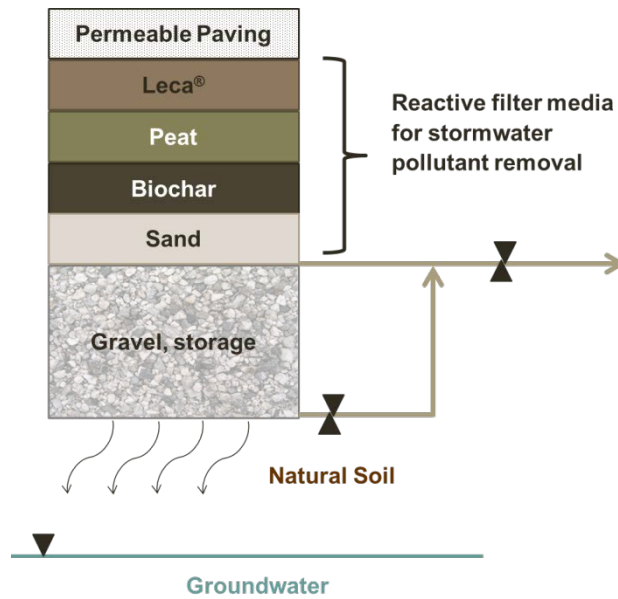


RESEARCH REPORT

VTT-R-05980-17
REPLACES RESEARCH REPORT VTT-R-05545-17






StormFilter Material Testing Summary Report

Performance of stormwater filtration systems

Authors: Laura Wendling, Kalle Loimula, Juhani Korkealaakso, Hannele Kuosa, Hanna Iitti and Erika Holt

Confidentiality: Public

Report's title	
StormFilter material testing summary report –performance of stormwater filtration systems	
Customer, contact person, address	Order reference
StormFilter project	
Project name	Project number/Short name
Engineering Infiltration Systems for Urban Stormwater Management - Reinventing Stormwater	106760/StormFilter
Author(s)	Pages
Laura Wendling, Kalle Loimula, Juhani Korkealaakso, Hannele Kuosa, Hanna Iitti, Erika Holt	49 p.
Keywords	Report identification code
Urban stormwater; Filter; Bio-based materials; Geomaterials	VTT-R-05980-17
Summary	
<i>This report is a corrected version that replaces research report no. VTT-R-05545-17.</i>	
<p>The geo- and bio-based materials used in green infrastructure are typically regarded as effectively inert with pollutant removal capacity limited to filtration of particulate materials; however, reactive filter material use in engineered stormwater management systems can provide substantial water quality benefits in passive and semi-passive stormwater treatment structures, and can provide fit-for-purpose treatment options for on-site runoff quality management. The present study examined copper, lead, zinc and phosphorus removal from a synthetic stormwater using several different bio- and geo-based filter materials in layered configuration or as a homogeneous mixture. All of the layered or mixed filter material systems examined herein effectively removed copper, lead, zinc, and phosphorus from stormwater. Coating of selected filter materials with iron oxides substantially improved phosphorus, and to a lesser extent zinc, retention. The rates of copper, lead, zinc and phosphorus removal obtained in these experiments were superior to or comparable with pollutant adsorption capacities of similar materials as reported in the scientific literature. The present work shows that with improved filter material designs based on well-understood, quantifiable mechanisms of contaminant removal, engineered stormwater infiltration systems have the potential to provide a reliable holistic stormwater management solution, yielding a water resource that is safe for aquifer recharge or to support healthy urban stream ecosystems. The results of the present study provide essential knowledge about the use of reactive filter media for stormwater treatment, facilitating the use of engineered infiltration or subsurface filtration media to manage not only stormwater quantity but also stormwater quality.</p>	
Confidentiality	Public
Espoo 3.11.2017	
Written by	Reviewed by
	
Laura Wendling Senior Scientist	Vesa Anttila Senior Scientist
	Accepted by
	
	Edgar Bohner Research Team Leader
VTT's contact address	
VTT Technical Research Centre of Finland Ltd, P.O. Box 1000, FI-02044 VTT, Finland	
Distribution (customer and VTT)	
StormFilter project group, VTT Oy, Aalto University, University of Helsinki	
<p><i>The use of the name of VTT Technical Research Centre of Finland Ltd in advertising or publishing of a part of this report is only permissible with written authorisation from VTT Technical Research Centre of Finland Ltd.</i></p>	

Executive Summary

The water storage and filtration potential of geo- and/or bio-based materials used in urban stormwater management infrastructure has not been fully exploited to date. The objective of the StormFilter project was to generate new technologies and business using bio- and mineral-based materials for stormwater purification by providing evidence for and quantifying mechanisms of pollutant removal by bio- and geo-based filter materials.

The present work utilised geomaterial and geochemical knowhow, along with experience from previous projects on pervious pavement, stormwater management with the urban green, biofiltration and stormwater monitoring and modelling to investigate pollutant attenuation by layers or mixtures of filter materials. Hydrogeochemical modelling was undertaken to further examine mechanisms of pollutant removal and inform interpretation of pollutant removal capacities, the relative long-term stability of pollutants retained within filter materials, and filter longevity.

Six different layered or homogeneously mixed filter systems were examined in laboratory column experiments:

1. 3–8 mm crushed Leca[®] / Peat + 10 wt.% limestone / Spruce biochar
2. 3–8 mm crushed Leca[®] / Peat + 10 wt.% limestone / Iron-treated spruce biochar
3. Iron-coated 3–8 mm crushed Leca[®] / Peat + 10 wt.% limestone / Spruce biochar
4. Homogeneous mixture of 10% spruce biochar - 90% 0–2 mm quartz sand
5. 3–8 mm crushed Leca[®] / Peat + 10 wt.% limestone
6. 3–8 mm crushed Leca[®] / Spruce biochar

Each layered or mixed system was also comprised of layers of KaM 0–5 mm aggregate above and below the filter materials shown above.

In addition, the 3–8 mm crushed Leca[®] / Peat + 10 wt.% limestone / Spruce biochar layered filter system, also containing KaM 0-5 mm aggregate layers, was scaled up and further tested on site using an infiltration rig. The capacity of layered or mixed systems of filter materials to attenuate the common stormwater pollutants copper, lead, zinc, and phosphorus from water was determined using a synthetic solution representative of a ten-fold concentrated 'first flush' of stormwater following a prolonged dry period. Results showed:

- The layered or mixed filter materials removed 81–97% of the total copper from influent stormwater. The three-layered system of 3–8 mm crushed Leca[®]/peat + 10 wt.% limestone/Fe-treated spruce biochar removed the greatest quantity of copper from influent stormwater, equivalent to 32.5 g/m³ or >97% of the total copper in influent stormwater.
- The layered or mixed filter materials removed 84–97% of the total lead from influent stormwater. Both the three-layered system of 3–8 mm crushed Leca[®]/peat + 10 wt.% limestone/Fe-treated spruce biochar and the homogeneous biochar-sand mixture removed >70 g lead/m³, equivalent to 97% of the total lead in influent stormwater.
- The layered or mixed filter materials removed 50–96% of the total zinc from influent stormwater. The layered Leca[®]/peat + 10 wt.% limestone/Fe-treated spruce biochar filter system removed the greatest quantity of zinc from influent stormwater, equivalent to 130 g/m³ or >96% of the total zinc in influent stormwater.
- The layered or mixed filter material systems showed moderate to good phosphorous attenuation in laboratory column tests with rates of phosphorus removal from 42–81%. The layered Leca[®]/peat + 10 wt.% limestone/Fe-treated spruce biochar filter system removed the greatest quantity of phosphorus from influent stormwater, equivalent to 25.2 g/m³ or >81% of the total phosphorus in influent stormwater.

- The up-scaled Leca[®]/peat + 10 wt.% limestone/ Spruce biochar filter system removed 87–99% of the copper, lead and zinc in influent stormwater, and >80% of the phosphorus.

Treatment of filter materials with iron significantly enhanced the retention of phosphorus, and to a lesser extent, zinc. Experimental results combined with geochemical modelling indicated that specific sorption to iron oxide/ (oxy)hydroxide mineral surfaces was a primary mechanism of metal and phosphorus (as phosphate) retention within filter media, along with the formation of a range of mineral precipitates. Of the pollutants retained by filter media, zinc was the most susceptible to potential re-mobilisation due to the relative strength of its association with solid surfaces.

The range of different filter materials available enables development of fit-for-purpose solutions to address a variety of site-specific conditions, such as existing soil characteristics, site conditions, anticipated or measured pollutant loads and expected rainfall based on local climate change forecasts. The solutions examined herein provide a basis for further development of tailored products for stormwater management.

Espoo 3.11.2017

Authors

Contents

Executive Summary	2
Contents.....	4
1. Introduction.....	5
2. Filter Material Selection	6
3. Laboratory Column Testing of Pollutant Removal	7
3.1 Design of Layered Columns.....	7
3.2 Influent Stormwater.....	8
3.3 Filter Material Layers and Mixtures	8
3.4 Results of Layered Column Experiments	10
3.4.1 Pollutant attenuation by two-phase filter systems.....	13
3.4.2 Pollutant attenuation by three-phase filter systems	17
4. Meso-Scale Stormwater Filter Testing of Pollutant Removal.....	19
4.1 Infiltration Rig Setup	19
4.2 Results of Meso-Scale Filter System Experiment.....	20
4.3 Geochemical Modelling of Treated Effluents.....	22
4.3.1 Aluminium Minerals.....	23
4.3.2 Iron Minerals.....	24
4.3.3 Manganese Minerals.....	25
4.3.4 Carbonate Minerals.....	26
4.3.5 Sulphate Minerals	27
4.3.6 Phosphate Minerals	27
4.3.7 Copper Minerals	28
4.3.8 Lead Minerals	29
4.3.9 Zinc Minerals	30
5. Discussion	31
5.1 Pollutant removal mechanisms	31
5.2 Implications for implementation.....	33
6. Conclusions	34
Appendix I. Results of column tests using layered filtration media.....	36
Appendix II. Results of meso-scale study using layered filtration media	37
Appendix III. Results of geochemical modelling of effluents from meso-scale study using layered filtration media.....	40

1. Introduction

Urban areas face the dual challenge of effectively managing water resources to minimize both flooding and freshwater scarcity whilst reducing greenhouse gas emissions and energy use. The hydro-meteorological consequences of climate change exacerbate the effects of soil sealing and increased runoff in urban areas, the overexploitation of available water resources, and ageing infrastructures, highlighting the need for new robust and reliable ways to manage flooding and improve the quality of surface runoff in order to protect vulnerable surface water bodies or to facilitate stormwater re-use when water is scarce. Flood events are expected to increase as a consequence of climate change and are particularly costly, accounting for two-thirds of the economic costs of damages attributed to natural disasters in Europe¹. Nearly 20% of European cities with >100 000 inhabitants are highly vulnerable to flooding².

In addition to increases in stormwater volume, urban water collection systems are also burdened by increasing urban populations. According to the Population Reference Bureau, by the year 2050, 84% of the world's population will be living in urban and suburban areas³. Cities must simultaneously ensure compliance with legislative guidelines to reduce risk to human populations and to improve ecological sustainability associated with the higher volumes of stormwater and its associated run-off pollutants^{4,5}. Stormwater management involves dealing with surface runoff following a precipitation event, and is essential in urban areas where surfaces are largely impermeable and infiltration is limited. Where stormwater is able to infiltrate soil, as in rural areas, it is filtered through the soil until it reaches an aquifer or flows into a surface water body. Runoff is the portion of precipitation that cannot infiltrate the soil surface, either because the infiltration capacity is exceeded as in a heavy rainfall event, or because the soil surface is sealed with impervious materials.

Urban systems of green infrastructure (rain gardens, green roofs, permeable pavements, swales, wetlands, etc.) designed to reduce stormwater runoff volume are identified in the EU Soil Sealing Guidelines as stormwater management solutions which enhance urban environments⁶. In combination with blue infrastructure, or urban landscape elements linked to water (lakes, ponds, waterways, etc.), green systems for urban stormwater management have gained popularity due to their cost effectiveness as well as the multiple co-benefits yielded by blue-green stormwater management systems. Green infrastructure systems often utilise engineered infiltration or subsurface filtration media to optimise hydraulic conductivity/maximise water infiltration, filter particulate pollutants or provide growth media for microbial communities. In general, urban green infrastructure is largely focused on filtration for stormwater quantity to minimise flooding, rather than water quality for pollution control.

¹ EEA 2012. Climate change, impacts and vulnerability in Europe 2012. EEA Report No 12/2012
<http://www.eea.europa.eu/media/publications/>

² EEA 2012. Water resources in Europe in the context of vulnerability. EEA Report No 11/2012
<http://www.eea.europa.eu/media/publications/>

³ Population Reference Bureau: <http://www.prb.org/educators/teachersguides/humanpopulation/urbanization.aspx>

⁴ HSY. 2010. Pääkaupunkiseudun ilmasto muuttuu. Sopeutumisstrategian taustaselvityksiä. HSY Helsingin seudun ympäristöpalvelut. HSY:n julkaisuja 3/2010. 92 p.

⁵ Kuntaliitto, 2012. Hulevesiopas. 298 s.

⁶ EC 2012. Guidelines on best practice to limit, mitigate or compensate soil sealing. European Union SWD(2012) 101.

The water storage and filtration potential of geo- and/or bio-based materials underlying green systems of infrastructure has not been fully exploited to date. The objective of the StormFilter project was to generate new technologies and business using bio- and mineral-based materials for stormwater purification. We sought to achieve this through an integration of blue-green-grey technologies: quantitative hydrologic and hydro-geochemical modelling to understand water quantity and quality under different design scenarios (blue); investigation of functional vegetation and landscape design alternatives (green); and geo- and bio-based filter material performance testing, including examination of fit-for-purpose material combinations (grey) (Figure 1).

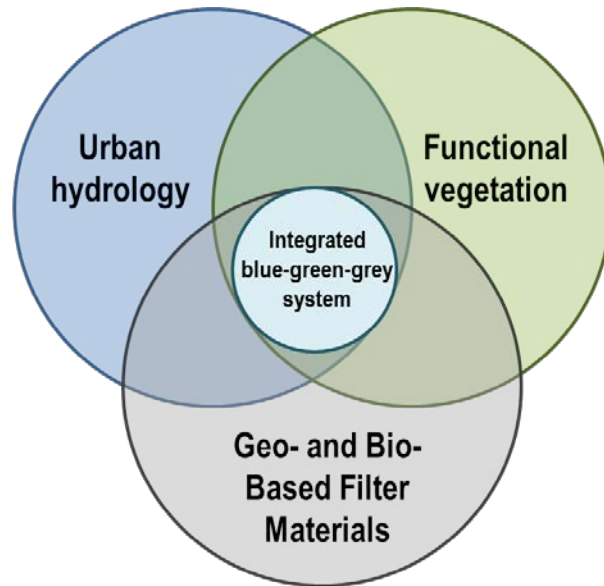


Figure 1. Conceptual diagram of StormFilter project structure, integrating blue-green-grey technologies for stormwater management.

2. Filter Material Selection

The geo- and bio-based materials used in green infrastructure are typically regarded as effectively inert with pollutant removal capacity limited to filtration of particulate materials. With improved filter material designs based on well-understood, quantifiable mechanisms of contaminant removal, engineered infiltration within integrated blue-green systems of urban stormwater management infrastructure has the potential to provide a reliable holistic stormwater management solution, yielding a water resource that is safe for aquifer recharge or to support healthy urban stream ecosystems.

Layered filter materials or geotechnical modules, as shown in Figure 2, may be integrated into infiltration and/or drainage systems in order to cost-effectively manage stormwater quality whilst at the same time controlling stormwater runoff quantity. The range of different filter materials available enables development of fit-for-purpose solutions to address a variety of site-specific conditions, such as existing soil characteristics, site conditions, anticipated or measured pollutant loads and expected rainfall based on local climate change forecasts. The solutions examined herein provide a basis for further development of tailored products for stormwater management.

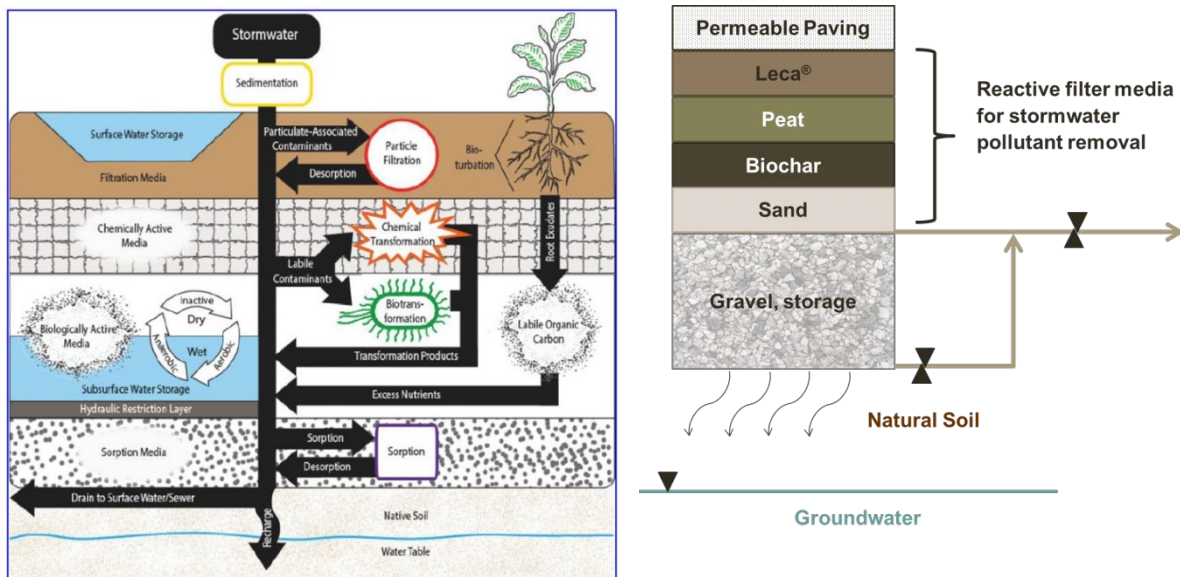


Figure 2. Schematic diagram of stormwater interaction with filter materials in an example filtration system (left). Conceptual model of an example layered system of filter materials beneath permeable pavement for stormwater quality management (right).

The present work utilised geomaterial and geochemical knowhow, along with experience from previous projects on pervious pavement, stormwater management with the urban green, biofiltration and stormwater monitoring and modelling^{7,8,9} to investigate pollutant attenuation by layers or mixtures of filter materials. Hydro-geochemical modelling was undertaken to further examine mechanisms of pollutant removal and inform interpretation of pollutant removal capacities, the relative long-term stability of pollutants retained within filter materials, and filter longevity. The improved understanding of material performance and mechanisms of attenuation for major pollutants in urban stormwaters is expected to support the development of new technologies and practices for improved urban stormwater management. This, in turn, is expected to generate new business for companies involved in material production, stormwater management structure design and/or implementation, and similar fields.

3. Laboratory Column Testing of Pollutant Removal

3.1 Design of Layered Columns

Layers or mixtures of test filter materials were placed in columns between layers of aggregate (Figure 3), including 40 mm of coarse aggregate and 150 mm of medium-fine aggregate, to normalize hydraulic retention time between materials with widely varying hydraulic conductivity as determined previously¹⁰. The purpose of the aggregate layers above and below test filter materials was to slow the flow of synthetic stormwater in highly porous materials with low hydraulic retention time, and to filter particulate materials.

⁷ Sänkiäho, L., Sillanpää, N. (Eds.) 2012. STORMWATER-hankkeen loppuraportti; Taajamien hulevesihaasteiden ratkaisut ja liiketoimintamahdollisuudet. Aalto-yliopiston julkaisusarja TIEDE+TEKNOLOGIA 4/2012. ISBN 978-952-60-4555-9. 60 p.

⁸ Sillanpää, N., Koivusalo, H. 2015. Impacts of urban development on runoff event characteristics and unit hydrographs across warm and cold seasons in high latitudes. J. Hydrol. 521:328–340.

⁹ Sillanpää, N., Koivusalo, H. 2015. Stormwater quality during residential construction activities: influential variables. Hydrol. Process. 29(19):4238–4251.

¹⁰ Wendling, L. et al. 2017. *StormFilter Material Testing Report. Localized performance of bio- and mineral-based filtration material components*. VTT Research Report VTT-R-01757-17. VTT Technical Research Centre of Finland, Espoo. 55 pp. http://www.vtt.fi/sites/stormfilter/Documents/VTT_R_01757_17_1708.pdf

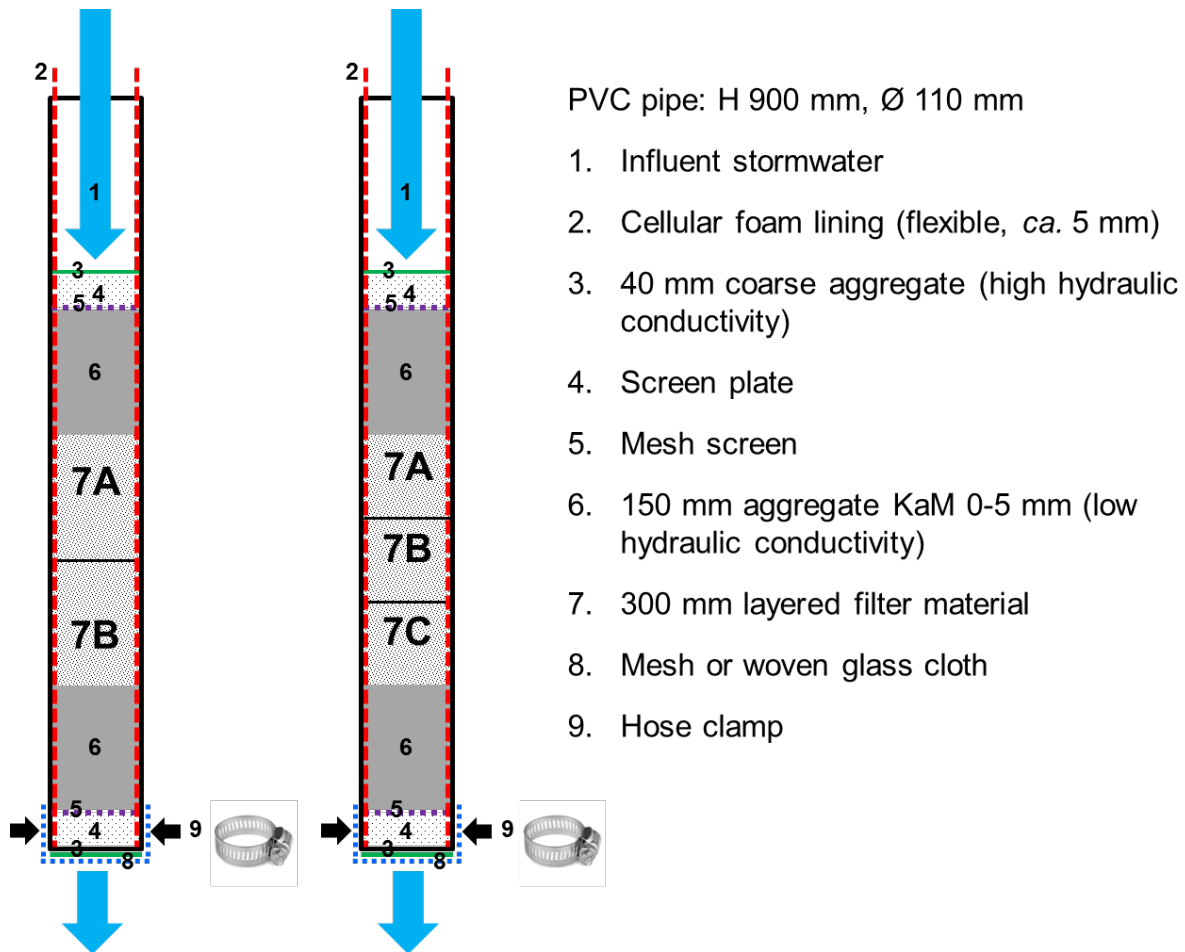


Figure 3. Configuration of StormFilter laboratory test columns for investigation of layered reactive filter materials, indicated here as no. 7. For the biochar-sand mixture, the middle 300 mm was comprised entirely of the 90 wt.% sand-10 wt.% biochar mixture.

3.2 Influent Stormwater

A synthetic stormwater of nominal 10X concentration relative to “average” European stormwater¹⁰ was used in column experiments (Table 1). The synthetic stormwater solution contained the common stormwater pollutants copper (Cu^{2+}), lead (Pb^{2+}), zinc (Zn^{2+}) and phosphorus (P^{5+} , as phosphate PO_4^{3-}), and was maintained at $\text{pH } 6,2 \pm 0,1$ to minimize the potential for *in situ* metal precipitation.

Table 1. Composition of synthetic stormwater used in laboratory column tests of layered materials. Concentrations expressed as mean value \pm one standard deviation from the mean.

	Concentration (mg/L)
Cu	5.13 \pm 0.95
Pb	11.4 \pm 3.73
Zn	20.7 \pm 0.82
Total P	4.72 \pm 0.54

3.3 Filter Material Layers and Mixtures

The combinations of individual filter materials for testing in mixtures or in a layered configuration were selected based on the results of previous laboratory testing, a survey of the scientific literature, and discussions with material producers. Test columns with multiple filter

materials contained one of the following within a 300-mm long section of the test column (with 150 mm KaM 0-5 mm aggregate above and below as shown in Figure 3): i) 100 mm each of three unique filter materials; ii) 150 mm each of two unique filter materials; or iii) a single 300 mm layer of mixed filter materials. The composition of filter material layers or mixtures is described in Table 2. Details of Leca[®], peat, and spruce biochar material characteristics are provided by Wendling et al. 2017¹⁰.

Table 2. Identity and configuration of filter materials within test columns.

ID	Contents	Composition of middle 300 mm length of column ^a
L-P-B	Leca [®] /Peat/Biochar	<ul style="list-style-type: none"> • 100 mm = Leca[®] crushed 3–8 mm • 100 mm = Peat + 10% limestone • 100 mm = Spruce biochar
L-P-FeB	Leca [®] /Peat/Fe-biochar	<ul style="list-style-type: none"> • 100 mm = Leca[®] crushed 3–8 mm • 100 mm = Peat + 10% limestone • 100 mm = Fe-treated spruce biochar
FeL-P-B	Fe-Leca [®] /Peat/Biochar	<ul style="list-style-type: none"> • 100 mm = Fe-coated crushed Leca[®] 3–8 mm • 100 mm = Peat + 10% limestone • 100 mm = Spruce biochar
10B-90S	Biochar-Sand	<ul style="list-style-type: none"> • 300 mm = 10% spruce biochar - 90% 0–2 mm quartz sand homogeneous mixture
L-P	Leca [®] /Peat	<ul style="list-style-type: none"> • 150 mm = Leca[®] crushed 3–8 mm • 150 mm = Peat + 10% limestone
L-B	Leca [®] /Biochar	<ul style="list-style-type: none"> • 150 mm = Leca[®] crushed 3–8 mm • 150 mm = Spruce biochar

^a Layered materials are listed in order from top (nearest the inlet) to bottom (nearest the outlet) of the column.

In addition to previously-tested filter materials, an iron-treated spruce biochar and iron-coated 3–8 mm crushed Leca[®] product were also utilised in tests of layered materials. Iron oxide treatment/ coating of materials may be employed to enhance removal of cations (Cu²⁺, Pb²⁺, Ni²⁺, Zn²⁺) in addition to some oxyanions (e.g. PO₄³⁻). The specifics of the coating procedure vary but the general principle is common^{11,12,13}. The coated material may first be acid-washed then rinsed with distilled water and dried prior to coating with iron. An iron containing solution, typically ferric nitrate (Fe(NO₃)₃) or ferric chloride (FeCl₃), is placed in contact with the solid material to be coated. The pH of the solution is increased using a concentrated chemical base such as NaOH to precipitate iron from the solution. Micro-scale iron precipitates form as a coating on the surfaces of the solid material. After some time, the solid material is rinsed with deionized water until the washing water is visually clear and only adhered iron oxide coating remains on the material surface. The precipitation and washing steps can be repeated several times to increase the quantity of iron coating on the final product. Finally, the coated material is dried prior to use.

In the present study, iron-treated spruce biochar for use in layered filter material systems was obtained directly from the material producer, RPK Hiili Oy (Mikkeli, Finland). Iron-coated Leca[®] was prepared in the laboratory by mixing 3–8 mm crushed Leca[®] material with 0.5 M Fe(NO₃)₃ at a solid to solution ratio of 1:4. The initially acidic solution (pH ca. 2) was adjusted to pH ≥10 using 3 M NaOH while stirring. The increase in solution pH catalysed the precipitation of poorly-crystalline iron oxide particulates from solution, a portion of which co-precipitated onto or

¹¹ Benjamin, M. et al. 1996. Sorption and filtration of metals using iron-oxide-coated sand. *Wat. Res.* 30(11):2609–2620.

¹² Gupta, V.K. et al. 2005. Adsorption of As(III) from aqueous solutions by iron oxide-coated sand. *J. Colloid Interf. Sci.* 288:55–60.

¹³ Lai, C.H., Chen, C.Y. 2001. Removal of metal ions and humic acid from water by iron-coated filter media. *Chemosphere*, Vol. 44, Issue 5, pp. 1177–1184.

adhered to Leca® material surfaces. The mixture was stirred continuously at 50 °C for 48 hours then oven-dried at 50 °C (Figure 4).

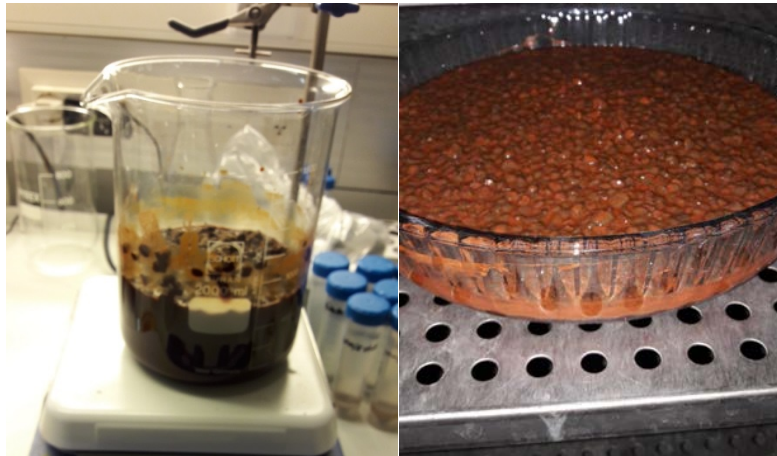


Figure 4. Leca® 3–8 mm crushed filter material was suspended in $\text{Fe}(\text{NO}_3)_3$ solution and the pH increased to ≥ 10 (left). After 48 hours, the material was oven-dried at 50 °C (right).

The dry material was washed with deionised water until the leachate was visually clear to remove non-adhered salts. Washed, Fe-coated Leca® materials were then oven dried at 50 °C to a constant mass prior to use in experiments (Figure 5).



Figure 5. Leca® materials treated with $\text{Fe}(\text{NO}_3)_3$ then oven dried were washed with deionised water (left) until the leachate was visually clear (right).

3.4 Results of Layered Column Experiments

All layered or mixed filter materials effectively removed metals from influent stormwater in laboratory column tests (Figure 6–Figure 8). All of the filter material systems tested removed >80% of the total copper from influent stormwater (Figure 6).

- The three-layered system of 3–8 mm crushed Leca®/peat with 10 wt.% limestone/Fe-treated spruce biochar (L-P-FeB) between layers of KaM 0–5 mm aggregate removed the greatest quantity of copper from influent stormwater, equivalent to 32.5 g/m³ or >97% of the total copper in influent stormwater.
- The three-layer system of Fe-coated Leca®/peat with 10 wt.% limestone/spruce biochar (FeL-P-B) removed 31.4 g/m³ or >94% of the total influent copper. In comparison, the Leca®/peat with 10 wt.% limestone/spruce biochar (L-P-B) system retained slightly less copper than the analogous system containing Fe-coated Leca® (FeL-P-B), with L-P-B removing 28.8 g/m³ or >86% of the total.

- Copper removal by layered Leca[®]-peat (L-P) was similar to L-P-B, with removal of 29.2 g/m³ or >87% of influent copper. In contrast, the Leca[®]-biochar (L-B) layered filtration system removed 27.0 g Cu/m³, or ca. 81% of total influent copper.
- The homogeneous mixture of 10 wt.% spruce biochar and 90 wt.% sand (10B-90S) removed 31.8 g/m³, or >95%, of the copper from influent stormwater.

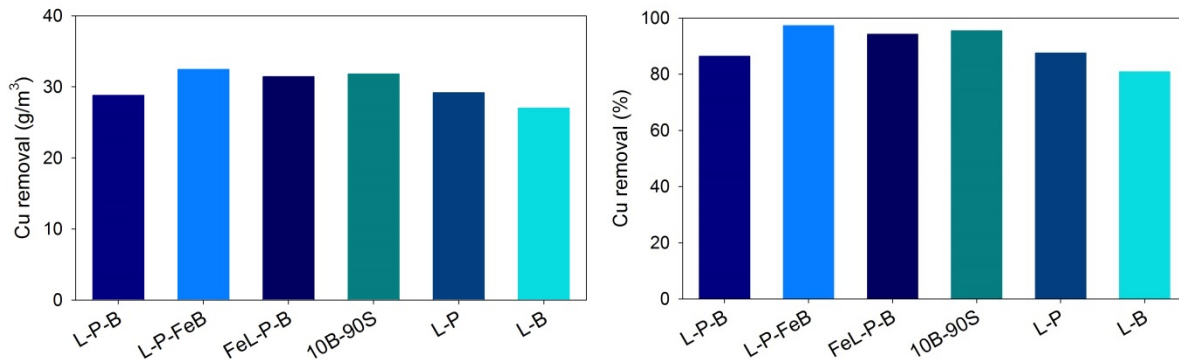


Figure 6. Overall copper (Cu) retention by layered filter materials in flow-through column testing, expressed in g/m³ (left) and as per cent of total (right).

All of the filter material systems tested removed >84% of the total lead from influent stormwater (Figure 7).

- The three-layered system of L-P-FeB removed the greatest quantity of lead from influent stormwater, equivalent to 70.7 g/m³ or >97% of the total lead in influent stormwater. This was similar to the performance of the homogeneous 10B-90S mixture filter, which removed nearly 70.3 g/m³, equivalent to 97%, of the lead from influent stormwater.
- The three-layer system of FeL-P-B removed 69.1 g/m³ or >95% of the total influent lead. In comparison, the L-P-B system retained less lead, 64.1 g/m³ or >88% of the total, than FeL-P-B.
- Lead removal by L-P was similar to L-P-B, with removal of 63.0 g/m³ or ca. 87% of influent lead. In contrast, the L-B layered filtration system removed 61.0 g Pb/m³, or ca. 84% of total influent lead.

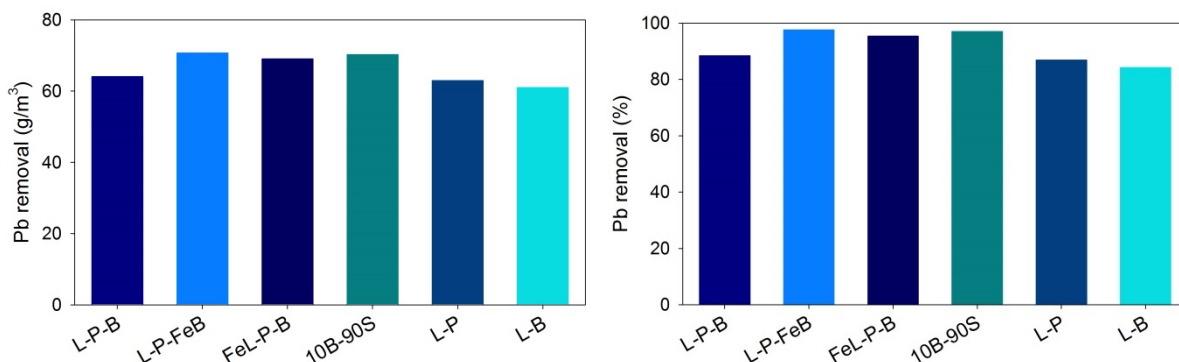


Figure 7. Overall lead (Pb) retention by layered filter materials in flow-through column testing, expressed in g/m³ (left) and as per cent of total (right).

Compared to copper and lead removal from stormwater, there was more clear differentiation between the filter systems with respect to zinc attenuation (Figure 8). All of the filter material systems tested removed at least 50% of the total zinc from influent stormwater.

- The three-layered system of L-P-FeB removed the greatest quantity of zinc from influent stormwater, equivalent to 130 g/m³ or >96% of the total zinc in influent stormwater.

- The three-layer system of FeL-P-B removed 106 g/m³ or 79% of the total influent zinc. This was similar to the performance of the homogeneous 10B-90S mixture filter, which removed 108 g/m³, equivalent to ca. 80%, of the zinc from influent stormwater.
- In comparison, the L-P-B system retained less zinc than either the FeL-P-B or the 10B-90S system, removing 94.4 g/m³ or 70% of the total zinc from influent stormwater. Zinc removal by L-P was similar to L-P-B, with removal of 96.2 g/m³ or ca. 71% of influent zinc.
- The L-B layered filtration system removed 67.3 g Zn/m³, or ca. 50% of total influent zinc.

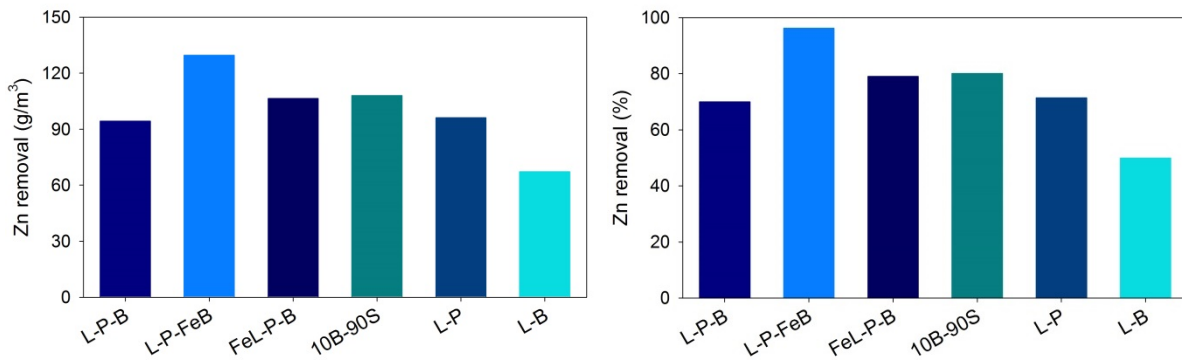


Figure 8. Overall zinc (Zn) retention by layered filter materials in flow-through column testing, expressed in g/m³ (left) and as per cent of total (right).

The layered or mixed filter material systems showed moderate to good phosphorous attenuation in laboratory column tests with rates of phosphorus removal from ca. 42–81% (Figure 9).

- Treatment of filter materials with iron significantly enhanced phosphorus retention. The L-P-FeB system removed the greatest quantity of phosphorus from influent stormwater, equivalent to 25.2 g/m³ or >81% of the total phosphorus in influent stormwater. The FeL-P-B removed 18.8 g/m³ or ca. 61% of the total influent phosphorus. In comparison, the L-P-B system retained substantially less phosphorus, 13.3 g/m³ or ca. 43% of the total, than the analogous systems containing Fe-coated Leca[®] or biochar.
- Phosphorus removal by layered L-P was similar to L-P-B, with removal of 12.8 g/m³ or nearly 42% of influent phosphorus. In contrast, the L-B layered filtration system removed 18.8 g P/m³, or nearly 61% of total influent phosphorus, similar to the FeL-P-B system.
- The 10B-90S mixture removed more phosphorus from influent stormwater than the FeL-P-B system, but less than the L-P-FeB system. The biochar-sand mixture removed 22.0 g/m³, or >71%, of the phosphorus from influent stormwater.

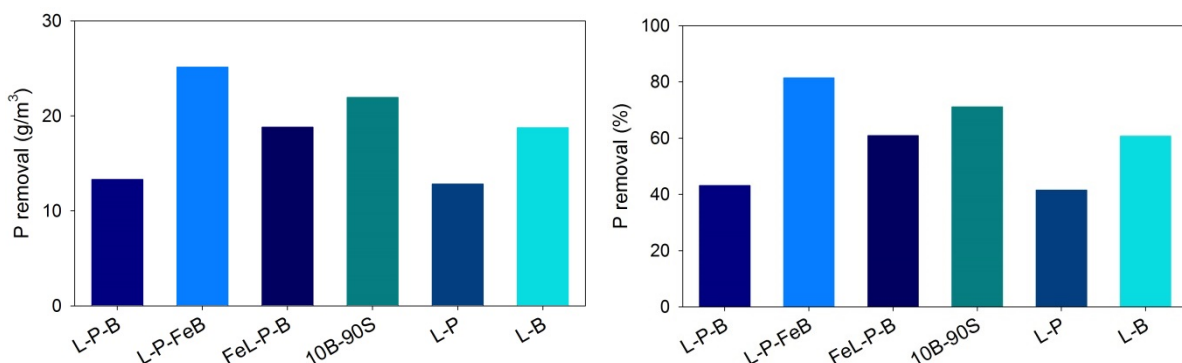


Figure 9. Overall phosphorus (P) retention by layered filter materials in flow-through column testing, expressed in g/m³ (left) and as per cent of total (right).

The figures above show overall pollutant retention by each filter material following passage of 37.5 L of synthetic stormwater solution through each respective column. Detailed plots in the following sub-sections show stormwater influent and column effluent pH, and concentrations of copper, lead, zinc and phosphorus (present as phosphate, PO_4^{3-}) in each respective column effluent as a function of time (expressed as effluent flux). Raw data from laboratory column experiments can be found in Appendix I.

3.4.1 Pollutant attenuation by two-phase filter systems

The pH of influent stormwater was maintained at 6.2 ± 0.1 throughout the experiment. Effluents from experimental columns containing layered Leca[®]/peat, Leca[®]/biochar or a homogeneous mixture of sand and biochar sand-biochar mixture remained higher than the influent pH (range 6.5–8.1) and showed a general decrease with time (Figure 10). The effluents from filter systems containing biochar were slightly higher than those of the Leca[®]-peat system, most likely due to the alkaline nature of the biochar solid. These results show that the two phase filter material systems, particularly those containing biochar, have capacity for acid neutralisation.

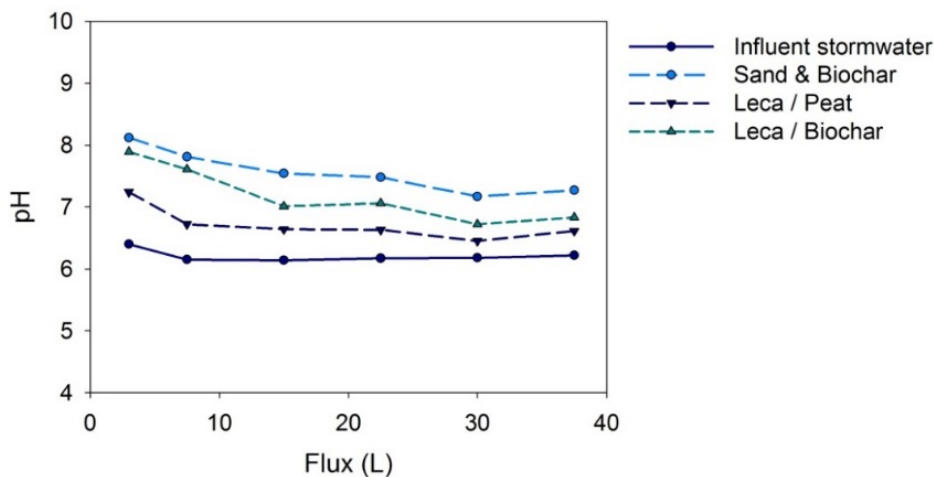


Figure 10. Influent stormwater pH and pH of effluents from columns containing two different filter materials.

Study of plots showing cumulative pollutant removal with time or, in this case, influent volume, helps provide an understanding of pollutant retention dynamics. Where cumulative pollutant retention increases by an approximately equal amount with each unit or time or influent volume, there is no apparent saturation of pollutant sorption sites. As the pollutant retention becomes incrementally lesser with each unit of time or volume it can be assumed that the filter material's capacity for pollutant removal is incrementally decreasing, e.g. the material is becoming incrementally less reactive towards the pollutant. A plot of pollutant retention versus time or volume shows a plateau, or stops increasing with each additional unit or time or influent volume, as an indication that the filter material's capacity for pollutant retention has been reached.

Of the two-phase filter systems investigated, only the Leca[®]-biochar filter system exhibited noticeable indication of decreased capacity for copper or lead retention during column trials (Figure 11, Figure 12). This trend is most evident in the plots showing per cent (%) copper or lead retained as a function of influent volume (flux). Neither copper nor lead retention capacity were reached in the Leca[®]-biochar filter system or either of the two other dual-phase filter systems examined in the present column experiments.

Copper, lead and zinc are typically considered soluble, strongly hydrated cations which are considered exchangeable and somewhat mobile in soil environments¹⁴ (which are analogous to the present filter systems). The alkaline pH of effluents from columns containing mixed sand and biochar, or layered Leca[®]-biochar or Leca[®]-peat indicates (Figure 10) the presence of acid-neutralizing ions, typically hydroxide (OH⁻), bicarbonate (HCO₃⁻) and/or carbonate (CO₃²⁻). Metals and phosphorus can react with carbonate minerals and subsequently be removed from solution through a combination of ion exchange and precipitation on carbonate mineral surfaces^{15,16}.

The solid-liquid partitioning of copper in soil porewaters (similar to the present filter systems) depends upon soil pH and organic matter content. Copper is most soluble at low pH and where organic matter content is low. Copper solid-solution chemistry is dominated by the formation of stable complexes with dissolved organic matter in organic-rich environments¹⁷. Herein, the organic matter content is assumed to be minimal as no external source of organic matter was provided. The potential organic matter content in test filter systems was limited to entrained trace particulate organic matter within solid media, which was not quantified in this study. Copper is known to strongly adsorb to manganese and iron oxide minerals in inorganic soils, forming strong complexes with manganese- and iron-hydroxyl functional groups on mineral surfaces¹⁷. In soils, the general order of copper adsorption to minerals: manganese oxides > organic matter > iron oxides > clay minerals¹⁸. In the two-phase filter systems examined (Figure 11) copper was most likely retained through ion exchange reactions or (co)precipitation with carbonates.

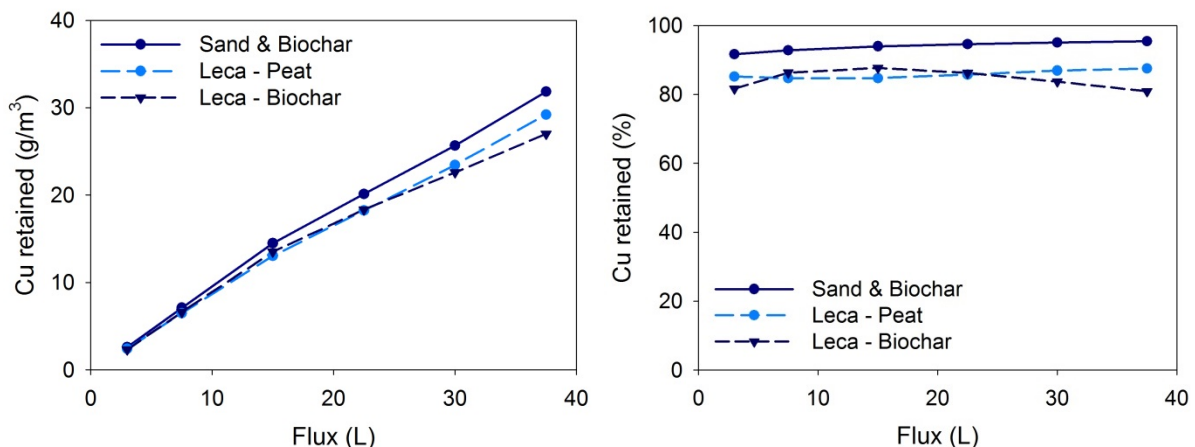


Figure 11. Cumulative copper (Cu) retention by layers of two different filter materials in flow-through column testing, expressed in g/m³ (left) and as per cent of total (right).

Similar to copper, lead is known to bind particularly strongly to organic matter at pH 4 and above in organic-rich soil environments, and to clay minerals and iron oxides in inorganic environments¹⁹. Where organic matter is present, lead transport depends primarily on the movement of lead-humic (organic matter) complexes²⁰. In addition, lead can replace calcium in carbonate minerals (e.g., through isomorphous substitution of Pb²⁺ for Ca²⁺ in CaCO₃) and

¹⁴ McBride, M.B. 1994. Environmental Chemistry of Soils. Oxford University Press, New York.

¹⁵ Zachara, J.M. et al. 1991. Sorption of divalent metals on calcite. *Geochim. Cosmochim. Acta* 55(6):1549–1562.

¹⁶ Wendling, L.A. et al. 2013. Phosphorus sorption and recovery using mineral-based materials: Sorption mechanisms and potential phytoavailability. *Appl. Geochem.* 37:1587–169.

¹⁷ Dixon, J.B., Weed, S.B. (Eds). 1989. Minerals in Soil Environments, 2nd Ed. Soil Science Society of America, Madison, WI.

¹⁸ Oorts, K. 2013. Copper. In, Alloway, B.J. (Ed.), Heavy Metals in Soils: Trace Metals and Metalloids in Soils and their Bioavailability, Environmental Pollution 22, Springer Science+Business Media, Dordrecht.

¹⁹ Steinnes, E. 2013. Lead. In, Alloway, B.J. (Ed.), Heavy Metals in Soils: Trace Metals and Metalloids in Soils and their Bioavailability, Environmental Pollution 22, Springer Science+Business Media, Dordrecht.

²⁰ Bergkvist, B. 1986. Leaching of metals from a spruce forest soil as influenced by experimental acidification. *Water Air Soil Poll.* 31:901–916.

has a strong affinity for sulphur. This characteristic – high affinity for sulphur phases – results in the concentration of lead in sulphur mineral phases in rocks, e.g. as in the mineral ore galena (PbS). In soil, lead is typically considered ‘fixed’ or immobile in the soil unless it is present at high concentrations²¹.

Sulphate in influent stormwater was low, including only that portion contributed by the local metropolitan drinking water supply used to make synthetic stormwater. Similarly, no external organic matter was introduced to the test columns so organic matter content was limited to trace quantities of organic matter possibly entrained within solid material phases. Like copper, in the two-phase filter systems examined (Figure 12) lead was most likely retained through ion exchange reactions or (co)precipitation with carbonates.

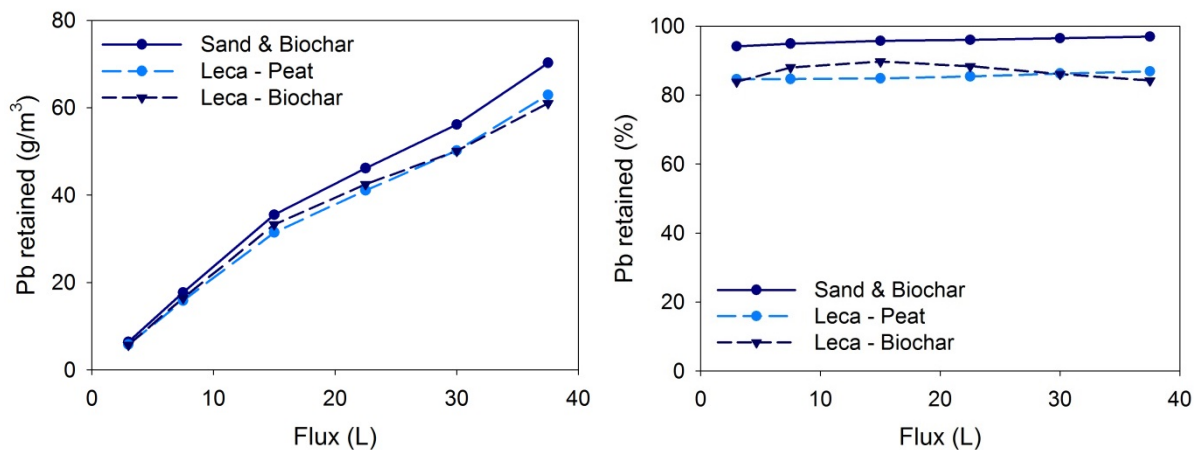


Figure 12. Cumulative lead (Pb) retention by layers of two different filter materials in column testing, expressed in g/m³ (left) and as per cent of total (right).

Knowledge of zinc behaviour and fate in soil environments assists with the interpretation of zinc dynamics in filter systems. Zinc behaviour is strongly influenced by solution pH, and its mobility is largely controlled by sorption-desorption reactions rather than precipitation-dissolution of zinc mineral phases²². Zinc is known to specifically adsorb to the pH-dependent binding sites of oxyhydroxide minerals and organic matter. When zinc is present at high concentrations it will also adsorb to clay mineral surfaces via ion exchange reactions. In general, zinc mobility increases with increasing pH. At low pH, the free ion Zn²⁺ is dominant and zinc can be expected to adsorb to iron, manganese and aluminium oxide and oxyhydroxide minerals and organic matter, or to clay mineral surfaces. As solution pH increases to >7, the ZnOH⁺ species dominates, whilst at pH >9 the dominant zinc species is Zn(OH)₂. Thus, with increasing solution pH, zinc is less likely to form specific surface complexes with oxyhydroxide minerals and organic matter. In the two-phase filter systems examined herein, zinc is most likely specifically adsorbing to trace particulate oxyhydroxides and organic matter, and non-specifically adsorbing to reactive clay mineral and biochar surfaces (Figure 13). The notable incremental decrease in per cent (%) zinc sorption with time in the Leca[®]-biochar system indicates that this filter system was likely beginning to approach zinc sorption capacity.

²¹ Tipping, E. et al. 2006. Simulating the long-term chemistry of an upland UK catchment: Heavy metals. Environ. Pollut. 141:139–150.

²² Mertens, J., Smolders, E. 2013. Zinc. In, B.J. Alloway (Ed.), Heavy Metals in Soils: Trace Metals and Metalloids in Soils and their Bioavailability, Environmental Pollution 22, Springer Science+Business Media, Dordrecht.

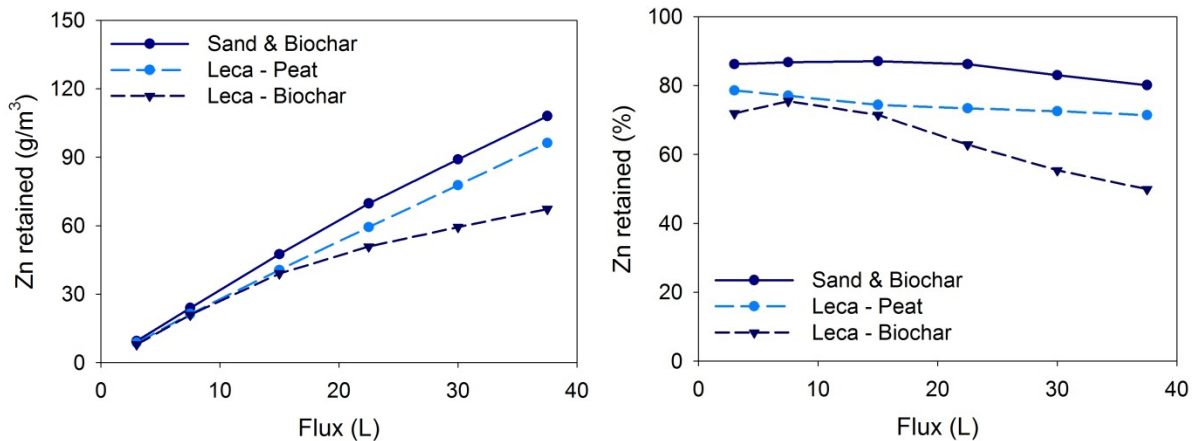


Figure 13. Cumulative zinc (Zn) retention by layers of two different filter materials in flow-through column testing, expressed in g/m^3 (left) and as per cent of total (right).

Figure 14 shows cumulative phosphorus retention by two-phase filter systems as a function of influent volume. In the present study, phosphorus was present at the phosphate molecule, PO_4^{3-} . Phosphate typically shows little sorption to clay minerals but strong specific sorption to iron, aluminium, zirconium and manganese (oxy)hydroxide minerals through both adsorption and surface precipitation reactions¹⁶. Iron oxides exhibit particularly high selectivity for phosphate, meaning that even trace quantities of iron oxide minerals can strongly affect phosphate behaviour.

Previous investigation of phosphate sorption to Leca[®] at pH 7 showed that the Leca[®] material adsorbed a relatively small amount of phosphate, most likely through phosphate sorption to Al-oxides²³. In general, biochar has little potential for phosphate removal from solution due to its surface chemistry. Most studies show limited phosphate retention by biochar²⁴, although previous work with the spruce biochar used herein demonstrated effective attenuation of phosphate in column trials using the spruce biochar as a single reactive phase¹⁰. Surface examination of biochar has shown the presence of colloidal and nano-scale MgO particles, which were determined to be the primary sites of phosphate adsorption²⁵. Biochars also typically contain a large quantity of calcium that may be released into solution. Another potential mechanism of phosphate removal from solution in filter systems containing biochar is the precipitation of calcium phosphate mineral phases.

²³ Johansson, L. 1997. The use of Leca (light expanded clay aggregate) for the removal of phosphorus from wastewater. *Water Sci. Technol.* 35(5):87–93.

²⁴ Yao, Y. et al. 2012. Effect of biochar amendment on sorption and leaching of nitrate, ammonium and phosphate in a sandy soil. *Chemosphere* 89(11):1467–1471.

²⁵ Yao, Y. et al. 2011. Removal of phosphate from aqueous solution by biochar derived from anaerobically digested sugar beet tailings. *J. Hazard. Mater.* 190:501–507.

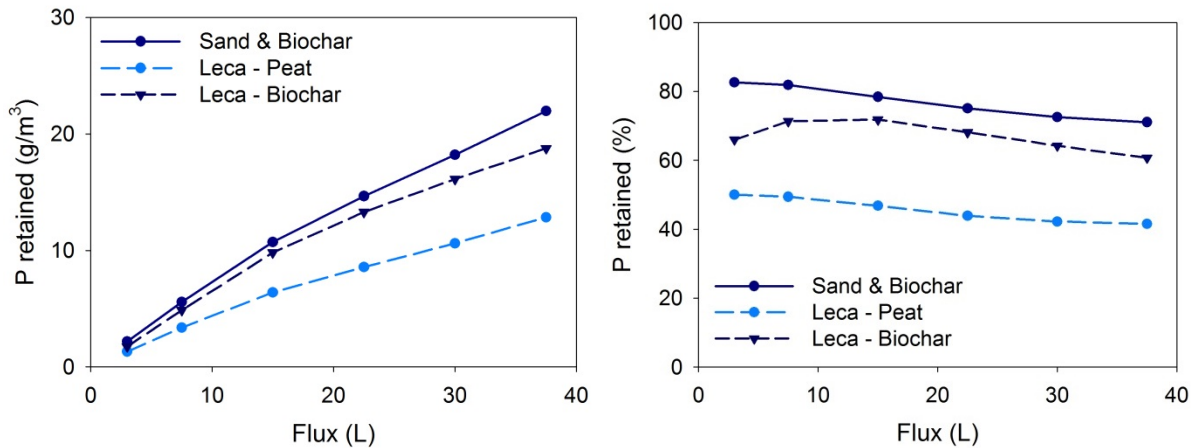


Figure 14. Cumulative phosphorus (P) retention by layers of two different filter materials in flow-through column testing, expressed in g/m^3 (left) and as per cent of total (right).

The relatively lesser adsorption of phosphate by the Leca[®]-peat filter system compared with filter systems containing biochar is most likely due to the capacity of peat for phosphate retention. The capacity of peat to remove phosphate from solution is largely dependent upon its amorphous iron and aluminium content. In previous work using phosphate concentrations ca. 1–2 mg/L peat has shown effective removal of phosphate from solution via sorption, with a sorption maxima of 8.9 g P/kg peat at pH 6.5²⁶. This was largely attributed to the formation of calcium-, iron, or aluminium-phosphates on peat surfaces. Each of the two-phase filter systems exhibited a notable decrease in incremental per cent (%) phosphorus removal from solution with time/ stormwater influent volume, which suggests that these systems were likely approaching their respective capacities for phosphorus retention.

3.4.2 Pollutant attenuation by three-phase filter systems

Similar to the two-phase stormwater filter systems examined, the pH of effluents from experimental columns containing three different filter materials in layered configuration was greater than that of the influent stormwater (Figure 15).

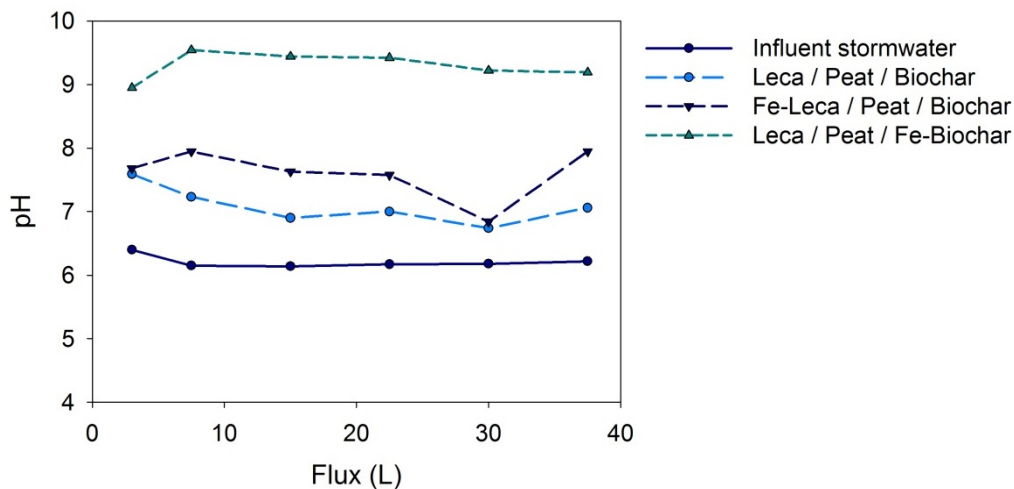


Figure 15. Influent stormwater pH and pH of effluents from columns containing three different filter materials.

²⁶ Xiong, J.B., Mahmood, Q. 2010. Adsorptive removal of phosphate from aqueous media by peat. *Desalination* 259:59–64.

Copper (Figure 16), lead (Figure 17) and zinc (Figure 18) were all effectively removed from influent stormwater and retained by each of the three-phase layered filtration systems. The Leca®/peat/biochar system exhibited slightly lesser attenuation of copper, lead and zinc relative to the filter systems containing an iron-treated material (e.g., either iron-coated Leca® or iron-treated biochar). In contrast to the two-phase filter systems studied, none of the filter systems containing three different materials exhibited a notable incremental decrease in copper, lead, or zinc retention with increasing time/stormwater influent volume.

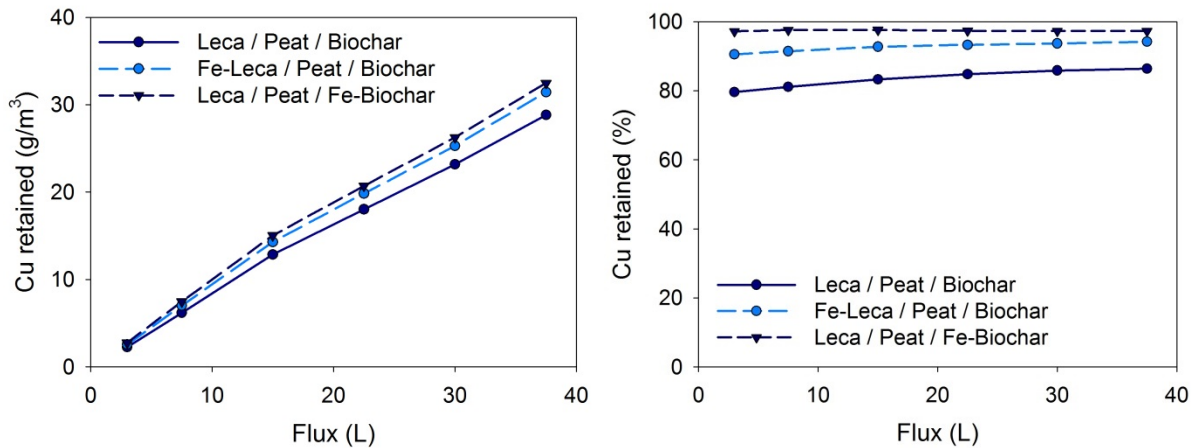


Figure 16. Cumulative copper (Cu) retention by layers of three different filter materials in flow-through column testing, expressed in g/m^3 (left) and as per cent of total (right).

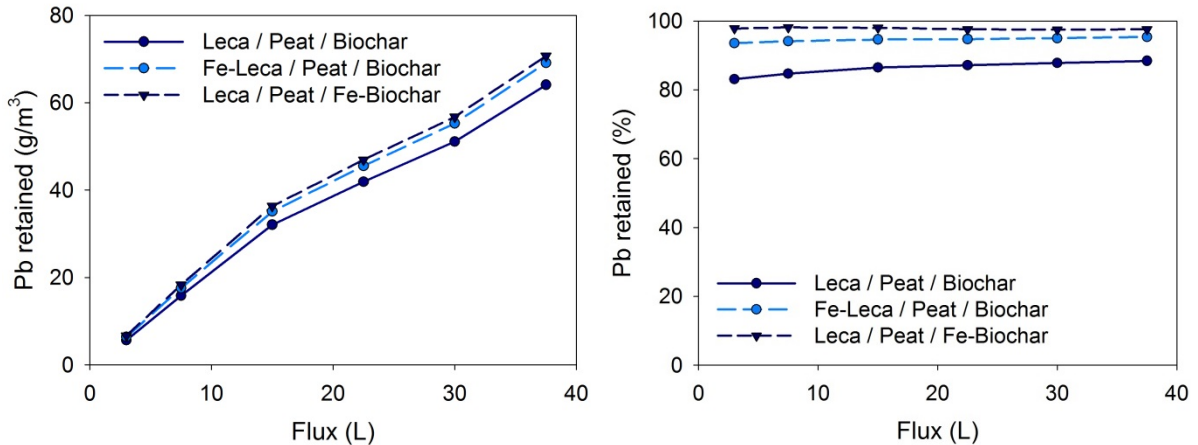


Figure 17. Cumulative lead (Pb) retention by layers of three different filter materials in flow-through column testing, expressed in g/m^3 (left) and as per cent of total (right).

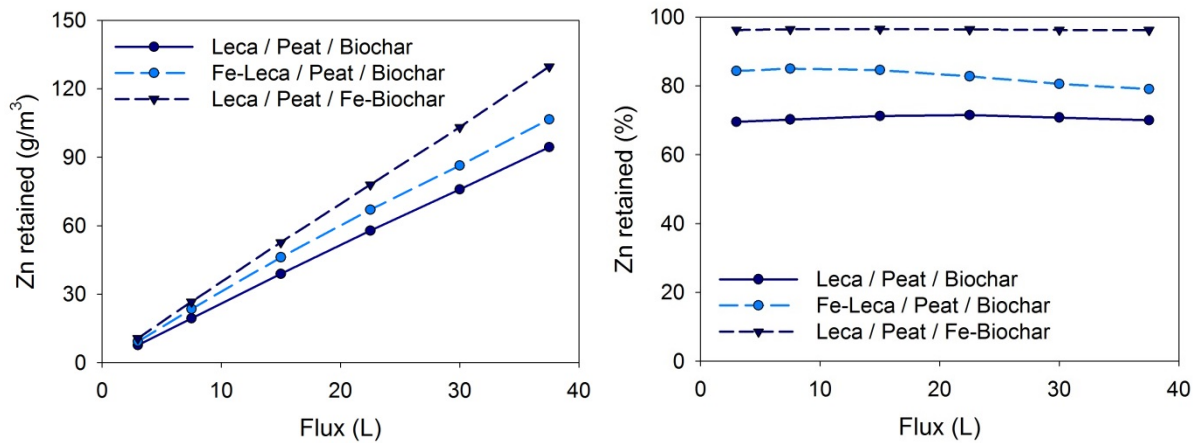


Figure 18. Cumulative zinc (Zn) retention by layers of three different filter materials in flow-through column testing, expressed in g/m^3 (left) and as per cent of total (right).

Phosphorus retention by three-phase filter systems (Figure 19) was similar to that observed for the two-phase filters (Figure 14), albeit with substantially greater net phosphorus retention by systems containing Fe-treated filter materials. The incremental decrease in phosphorus retention with increasing time/ influent stormwater volume suggests that the filter systems were likely slowly approaching their respective phosphorus retention capacities.

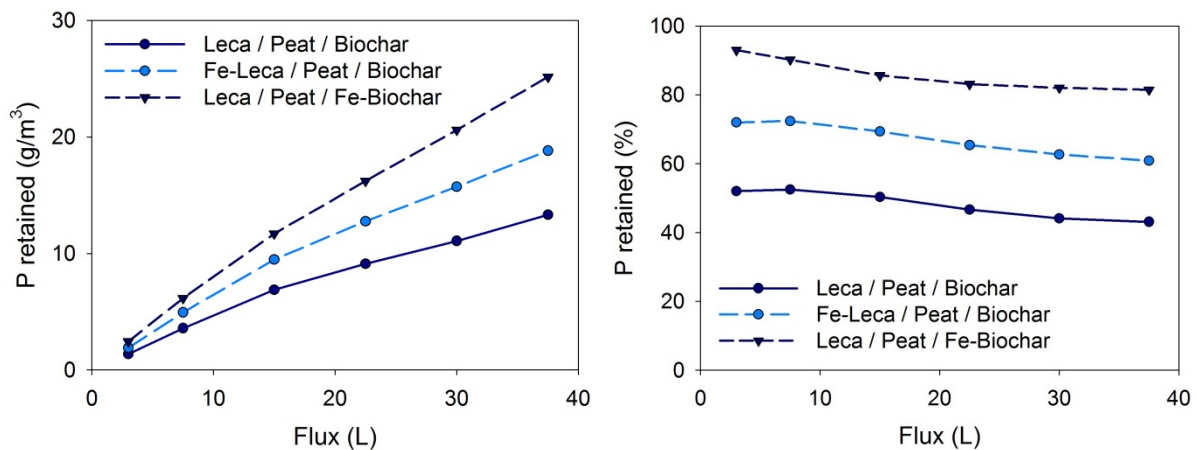


Figure 19. Cumulative phosphorus (P) retention layers of three different filter materials in flow-through column testing, expressed in mg/kg (left), g/m^3 (middle), and as per cent of total (right).

4. Meso-Scale Stormwater Filter Testing of Pollutant Removal

4.1 Infiltration Rig Setup

The performance of layered filter materials was further examined in a meso-scale infiltration rig using 3–8 mm crushed Leca®, peat with 10 wt.% limestone, and spruce biochar. The filter materials were configured within the infiltration rig in a layered configuration similar to the L-P-B column examined in previous experiments (Figure 3, Table 2):

- Top 50 mm = coarse aggregate with high hydraulic conductivity
- 150 mm = KaM 0–5 mm aggregate

- 100 mm = Leca crushed 3–8 mm
- 100 mm = Peat + 10% limestone
- 100 mm = Spruce biochar
- 150 mm = KaM 0–5 mm aggregate
- Bottom 150 mm = coarse aggregate with high hydraulic conductivity.

The total volume of solid material within the infiltration rig was 0.45 m³ (Figure 20). The ‘reactive filter phase’ was comprised of a 0.3 m³ section in the centre of the material comprised of 3–8 mm crushed Leca®, peat with 10 wt.% limestone, and spruce biochar between layers of KaM 0-5 mm aggregate. Synthetic stormwater (Table 1) was added to the infiltration rig in 25 L aliquots distributed evenly across the surface of the filter system. Effluents were discharged from the base of the infiltration rig and collected for analysis.

In comparison to the column experiments described previously (section 3), the meso-scale experiment conducted using the infiltration rig was performed on a >50X greater scale. The volume of reactive filter material in column experiments was 0.0057 m³ whereas the volume of reactive filter material in the infiltration rig experiment was 0.3 m³. Note that although the volume of filter material was >50X greater in the infiltration rig experiment compared with column trials, the volume of stormwater added per aliquot was <17X greater. In the column trials, each aliquot of stormwater added to layered filter systems was 1.5 L whilst stormwater was added to the infiltration rig in 25 L aliquots. Raw data from the meso-scale infiltration rig study can be found in Appendix II.

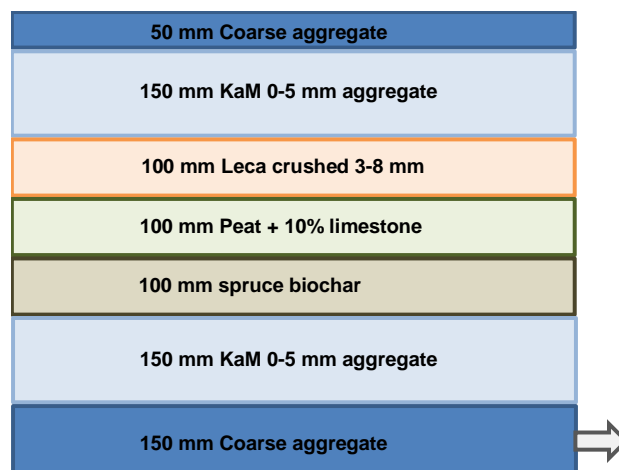


Figure 20. Conceptual diagram of layered filter media within infiltration rig. Infiltration rig dimensions 1.0 m L x 0.5 m W x 0.9 m H.

4.2 Results of Meso-Scale Filter System Experiment

Despite lesser absolute values for phosphorus, copper, lead and zinc removal from influent stormwater on a volume basis (Figure 21), the pollutant removal efficiency of layered 3–8 mm crushed Leca®/peat with 10 wt.% limestone/spruce biochar filter materials was superior in scaled-up infiltration experiment compared with the analogous column experiment (Figure 6–Figure 9). The difference in absolute pollutant retention (i.e. g/m³ values) was due to the lesser total quantity of pollutants delivered in influent stormwater per unit volume of filter media in the infiltration rig experiment.

- More than 97% of the total copper in the influent stormwater, or 10.7 g Cu/m³ filter material, was retained in the meso-scale infiltration rig experiment (Figure 21). In contrast, in column trials the Leca®/peat with 10 wt.% limestone/spruce biochar (L-P-B) system removed 57.7 g/m³ or >86% of the total copper from influent stormwater (Figure 6).

- Nearly all lead was removed from influent stormwater in the infiltration rig experiment (Figure 21). Lead removal in the infiltration rig experiment was equivalent to 26.7 g Pb/m^3 , or 99.7% of the total. In column trials, the L-P-B system retained 128 g/m^3 or >88% of the total lead in influent stormwater (Figure 7).
- The up-scaled filter system tested in the infiltration rig removed >87% of the total zinc from influent stormwater (Figure 21), a quantity equivalent to 39.4 g/m^3 . In comparison, in column trials, the L-P-B layered system removed 189 g/m^3 or 70% of the total zinc from influent stormwater (Figure 8).
- Phosphorous attenuation was >80% in the infiltration rig experiment; ca. 8.4 g P/m^3 was retained in the meso-scale experiment (Figure 21). In column trials, the L-P-B system retained substantially less phosphorus, 26.6 g/m^3 or ca. 43% of the total in influent stormwater (Figure 9).

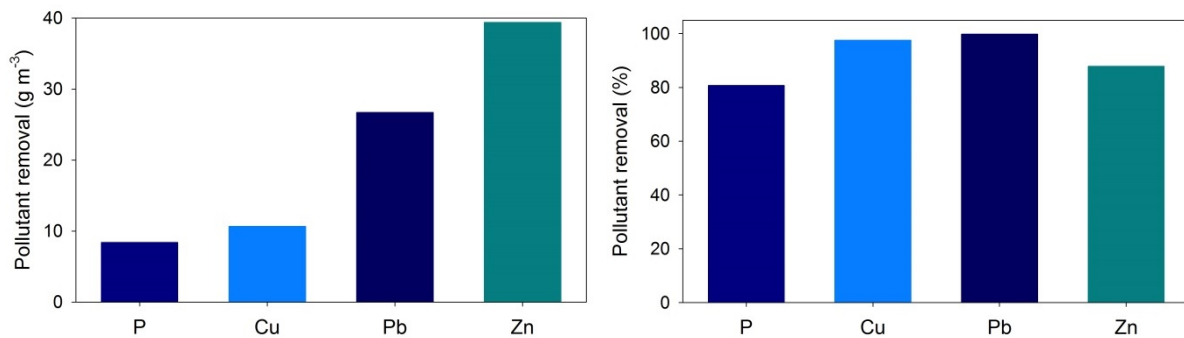


Figure 21. Overall phosphorus (P), copper (Cu), lead (Pb) and zinc (Zn) retention by layered filter materials in meso-scale tests using 10X concentrated synthetic stormwater, expressed in grams per m³ (left) and as per cent of total (right).

Examination of cumulative pollutant retention as a function of time, here represented as stormwater flux, shows consistently high rates of removal for copper, lead, zinc, and phosphorus in the infiltration rig experiment (Figure 22). In particular, rates of copper and lead attenuation in the up-scaled experiment showed high removal efficiency which was sustained throughout the duration of the experiment. The rates of both zinc and phosphorus removal in the infiltration rig experiment show a slight decline with time (Figure 22), but both zinc and phosphorus removal rates remain substantially greater than those exhibited by the L-P-B layered filter system in column trials (Figure 18, Figure 19).

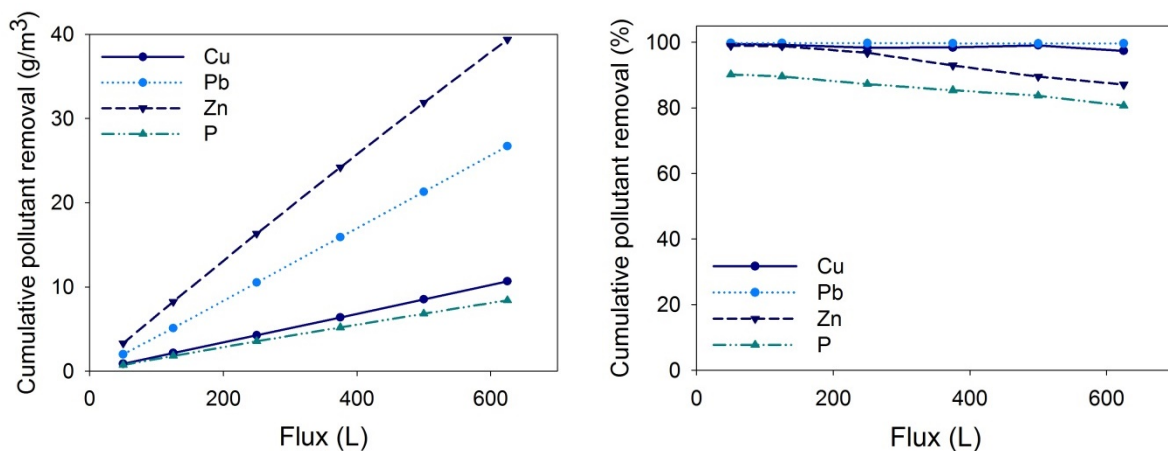


Figure 22. Cumulative phosphorus (P), copper (Cu), lead (Pb) and zinc (Zn) retention by layered filter materials in meso-scale tests as a function of stormwater flux, expressed in grams per m³ (left) and as per cent of total (right).

The pH of effluent from the meso-scale layered L-P-B filter system in the infiltration rig experiment (Figure 23) was similar to the pH of effluent from the L-P-B column (Figure 15).

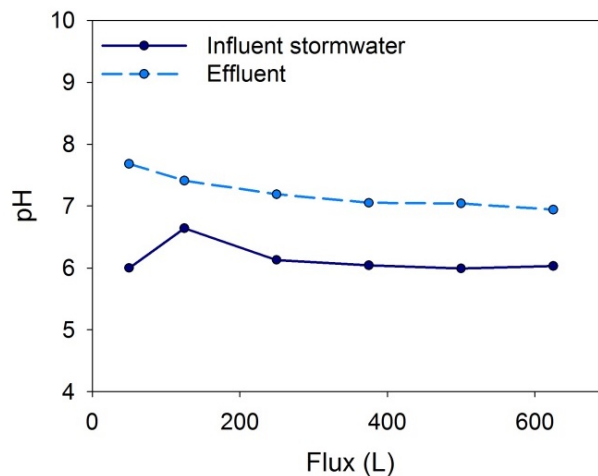


Figure 23. Influent stormwater pH and pH of effluent from infiltration rig containing layered 3–8 mm crushed Leca[®]/peat with 10 wt.% limestone/spruce biochar filter media.

4.3 Geochemical Modelling of Treated Effluents

Effluents from the infiltration rig meso-scale stormwater filtration experiment were collected and analysed for pH, electrical conductivity (EC), total alkalinity, dissolved carbon content, and selected cations and anions, including Al³⁺, Ca²⁺, Fe²⁺, Mg²⁺, Mn²⁺, K⁺, Na⁺, Si⁴⁺, P⁵⁺, Cu²⁺, Pb²⁺, Zn²⁺, Cl⁻ and SO₄²⁻. Geochemical modelling using the PHREEQC hydro-geochemical transport model was carried out on effluents from the infiltration rig meso-scale stormwater filtration experiment to inform interpretation of the solute geochemistry. PHREEQC Interactive Version 3.3.3²⁷ was used to model the hydro-geochemistry of major ions Na⁺, K⁺, Ca²⁺, Mg²⁺, Cl⁻, HCO₃⁻, SO₄²⁻ as well as Fe²⁺, Al³⁺, Mn²⁺, P⁵⁺, Cu²⁺, Pb²⁺, and Zn²⁺. Saturation indices (SIs) of mineral phases were estimated using PHREEQC calculations. Model input parameters were sourced from the minteq.v4 database.

Geochemical modelling uses thermodynamic principles to provide an indication of the geochemical equilibrium reactions controlling the concentration of dissolved constituents. A positive saturation index (SI) value (SI >0) indicates that the solution is supersaturated with respect to a given solid phase, and that the solid (mineral) may precipitate as a secondary phase. A negative SI value (SI <0) indicates that a given mineral phase is undersaturated with respect to the solution, not stable, and may dissolve if the undersaturated mineral phase is present in solid material which is in contact with the solution. Due to uncertainties, where the SI is ± one standard deviation from the mean for a given mineral phase is between -0.5 and 0.5, the solution is assumed to be in thermodynamic equilibrium with respect to that solid phase.

Variations in the infiltration rig meso-scale stormwater filter effluent pH and the saturation indices of major aluminium, iron, manganese and carbonate (CO₃), sulphate and phosphate minerals as a function of cumulative flux of stormwater through the infiltration rig, along with the saturation indices of clay minerals, amorphous Si (SiO_{2(am)}) and copper, lead and zinc mineral phases as a function of cumulative flux of stormwater through the infiltration rig are shown below.

²⁷ Parkhurst, D.L., Appelo, C.A.J. 2013. Description of input and examples for PHREEQC version 3 - A computer program for speciation, batch-reaction, one-dimensional transport, and inverse geochemical calculations. United States Department of the Interior, Washington, DC.

A comprehensive list of modelled mineral phases and their respective SI as a function of time/ stormwater flux can be found in Appendix III.

4.3.1 Aluminium Minerals

The $\text{Al}_2\text{O}_3\text{-SO}_3\text{-H}_2\text{O}$ system aqueous geochemistry is complex due to the large number of minerals that may form across a wide range of pH and sulphate concentrations. Aluminium concentrations in natural waters are typically controlled by gibbsite ($\text{Al}(\text{OH})_3$) and kaolinite ($\text{Al}_2\text{Si}_2\text{O}_5(\text{OH})_4$) due to the low solubilities of these minerals²⁸. Non-crystalline Al hydroxide ($\text{Al}(\text{OH})_{3(\text{am})}$) is least soluble between pH ca. 5–7; crystalline $\text{Al}(\text{OH})_3$ as gibbsite extends aluminium hydroxide insolubility across a wider pH range. Aluminium which precipitates initially as an amorphous Al hydroxide over time develops a more ordered structure to become the mineral gibbsite.

The presence of sulphate along with Al in aqueous solution can result in the formation of minerals such as alunite ($\text{KAl}_3(\text{SO}_4)_2(\text{OH})_6$), jurbanite (AlSO_4OH) or basaluminite ($\text{Al}_4\text{SO}_4(\text{OH})_{10}\cdot 5\text{H}_2\text{O}$). Evidence for jurbanite (AlSO_4OH) formation of in the natural environment is limited, and basaluminite and/or alunite generally control aluminium solubility in sulphate-rich natural waters²⁹. Precipitation of an amorphous basaluminite from solutions rich in aluminium and sulphate has been shown, followed by basaluminite transformation with time to the mineral alunite where alkali metals and a suitable catalyst were present³⁰. Geochemical modelling of infiltration rig meso-scale stormwater filter effluents showed that the aluminium minerals gibbsite, kaolinite and boehmite ($\gamma\text{-AlOOH}$) were theoretically oversaturated in filter effluents (Figure 24). Aluminium sulphate minerals alunite and basaluminite were transiently oversaturated, exhibiting increasing theoretical oversaturation with time. Jurbanite remained highly undersaturated throughout the experiment.

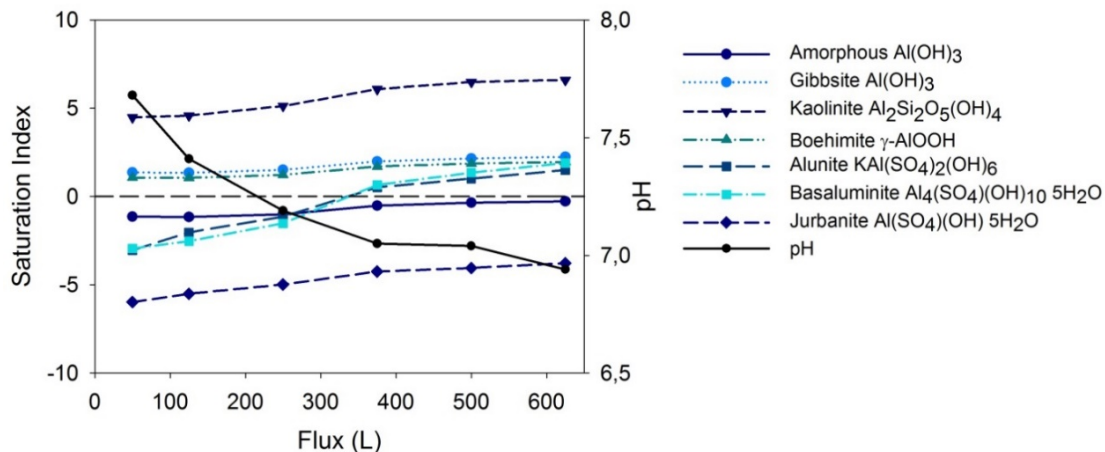


Figure 24. Change in saturation indices (SI) of major aluminium mineral phases in infiltration rig meso-scale stormwater filter with increasing stormwater influent flux.

Gibbsite and alunite are the most theoretically stable aluminium minerals at alkaline pH; however, the formation of crystalline aluminium sulphate minerals is kinetically slow. Therefore, precipitation of amorphous basaluminite is likely even when alunite or gibbsite is theoretically a more stable mineral phase³⁰. Geochemical modelling showed that the hydroxy-aluminium phases kaolinite, gibbsite and boehmite were theoretically oversaturated in infiltration rig effluents. Amorphous aluminium hydroxide ($\text{Al}(\text{OH})_{3(\text{am})}$) was initially undersaturated and approached saturation as the experiment progressed. A high degree of

²⁸ Hem, J.D. 1970. Aluminum-abundance in natural waters and in the atmosphere. In, Wedepohl, K.H. (Ed.) Handbook of Geochemistry Vol. II-2, Section 13-1. Springer-Verlag, Berlin.

²⁹ Adams, F., Hajek, B.F. 1978. Effects of solution sulphate, hydroxide, and potassium concentrations on the crystallization of alunite, basaluminite, and gibbsite from dilute aluminium solutions. Soil Sci. 126:169–173.

³⁰ Nordstrom, D.K. 1982. The effect of sulphate on aluminium concentrations in natural waters: some stability relations in the system $\text{Al}_2\text{O}_3\text{-SO}_3\text{-H}_2\text{O}$ at 298 K. Geochim. Cosmochim. Acta 46:681–692.

neof ormation of crystalline minerals is unlikely during the relatively short period of meso-scale infiltration rig filter operation, making amorphous Al hydroxide the mineral phase most likely controlling Al solubility in stormwater filter effluents despite its initial theoretical undersaturation and lesser degree of saturation relative to other hydroxy-aluminium mineral phases.

4.3.2 Iron Minerals

Ferrihydrite (amorphous $\text{Fe}(\text{OH})_3$), goethite ($\alpha\text{-FeOOH}$), hematite ($\alpha\text{-Fe}_2\text{O}_3$), lepidocrocite ($\gamma\text{-FeOOH}$) and schwertmannite ($\text{Fe}_8\text{O}_8(\text{OH})_6(\text{SO}_4) \cdot n\text{H}_2\text{O}$) were all oversaturated in the infiltration rig effluents throughout the experiment (Figure 25). Oversaturation of these mineral phases is likely largely due to the presence of exchangeable Fe^{2+} on solid filter material surfaces and soluble iron (Fe^{2+}) in influent water. All forms of iron (hydr)oxides are highly insoluble in aqueous solution³¹ so even a very small quantity of iron in solution will likely precipitate with time.

Ferrihydrite (amorphous $\text{Fe}(\text{OH})_3$) is a poorly crystalline, metastable hydrated iron oxide which forms by rapid hydrolysis of Fe^{3+} salts or rapid oxidation of solubilised Fe^{2+} , and is the precursor to more crystalline iron oxides such as goethite ($\alpha\text{-FeOOH}$), hematite ($\alpha\text{-Fe}_2\text{O}_3$) and lepidocrocite ($\gamma\text{-FeOOH}$). Formation of hematite is favoured between pH ca. 6 to 9, whilst goethite forms preferentially at higher and lower pH. The transformation of ferrihydrite to goethite or hematite has been shown to be strongly retarded by the presence of silica ions which modify ferrihydrite solubility, surface area and dehydroxylation behaviour³². Lepidocrocite is a polymorph of goethite and forms under similar conditions. In natural waters, iron oxyhydroxide precipitates initially consist of amorphous material, goethite, and sometimes lepidocrocite³³.

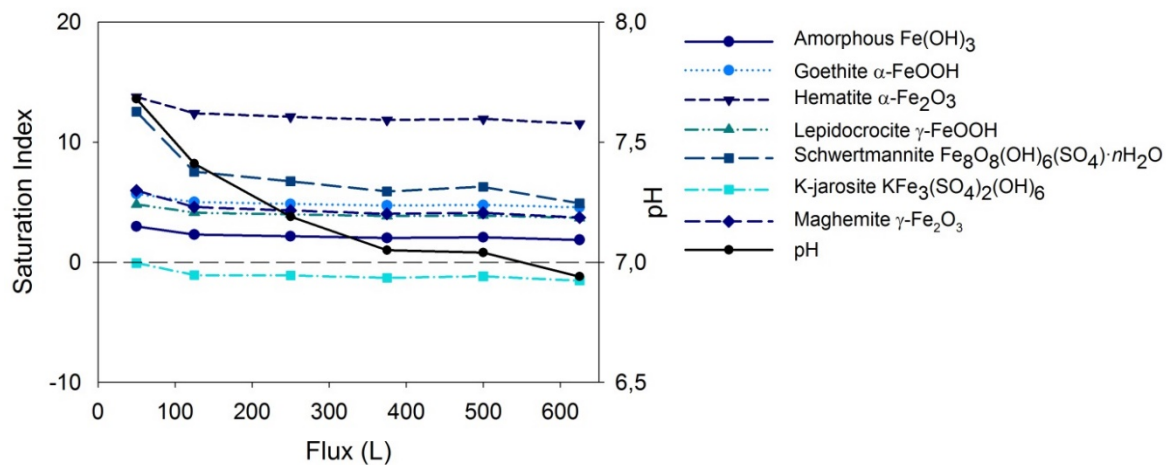


Figure 25. Change in saturation indices (SI) of major iron mineral phases in infiltration rig meso-scale stormwater filter with increasing stormwater influent flux.

The iron carbonate mineral siderite (FeCO_3), along with the iron phosphate mineral vivianite ($\text{Fe}_3(\text{PO}_4)_2 \cdot 8\text{H}_2\text{O}$) and iron sulphate mineral sodium jarosite ($\text{NaFe}_3(\text{SO}_4)_2(\text{OH})_6$) remained undersaturated throughout the meso-scale stormwater infiltration study (data not shown). In contrast, potassium jarosite ($\text{KFe}_3(\text{SO}_4)_2(\text{OH})_6$) was initially at approximate equilibrium with the solution phase, most likely due to an initial release of potassium ions (K^+) from surface exchange sites and a concomitant increase in K^+ solution concentration (Figure 26).

³¹ Schwertmann, U., Taylor, R. M. 1977. Iron oxides. Pp. 145-180 in, Dixon, J.B., Weed, S.B. (Eds.), Minerals in Soil Environments, Soil Science Society of America, Madison, WI.

³² Cornell, R.M. et al. 1987. Effect of silicate species on the transformation of ferrihydrite into goethite and hematite in alkaline media. Clays Clay Miner. 35:21-28.

³³ Langmuir, D., Wittermore, D.O. 1971. Variations in the stability of precipitated ferric oxyhydroxides. Pp. 209-234 in Hem, J.D. (Ed.) Nonequilibrium Systems in Natural Water Chemistry Volume 106. American Chemical Society, Washington, DC.

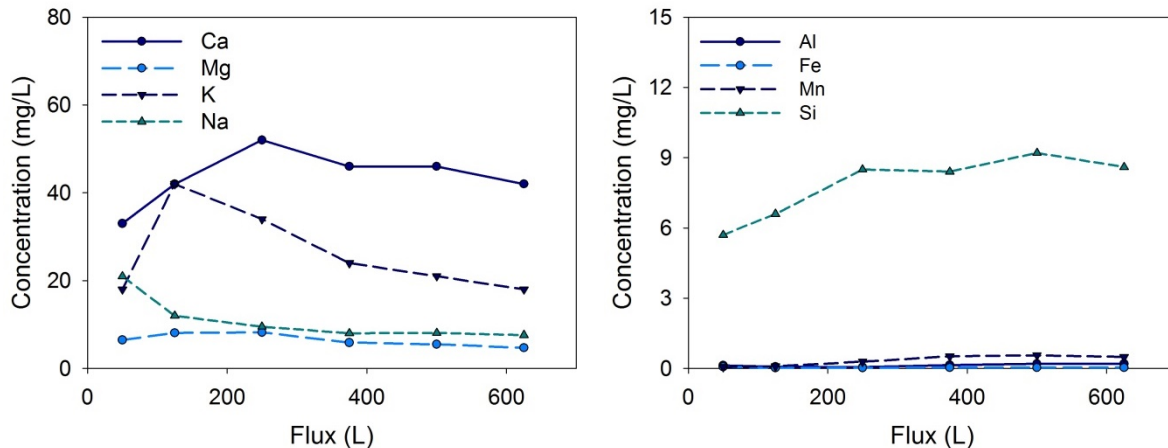


Figure 26. Major cations in effluents from infiltration rig meso-scale stormwater filter with increasing stormwater influent flux.

Maghemite ($\gamma\text{-Fe}_2\text{O}_3$) was theoretically oversaturated throughout the meso-scale stormwater infiltration study (Figure 25), as was magnetite (Fe_3O_4 ; data not shown). Magnetite is rarely identified in the natural environment, but is readily synthesised in laboratory experiments. The scarcity of magnetite identification in nature may be due to its tendency to oxidise to form maghemite, which is itself a dimorph of hematite³¹.

The Fe(III)-oxyhydroxysulphate mineral schwertmannite ($\text{Fe}_8\text{O}_8(\text{OH})_6(\text{SO}_4) \cdot n\text{H}_2\text{O}$) may form at acidic pH (e.g. pH 3.0–4.5) and where sulphate is present at concentrations of approximately 1.000 to 3.000 mg/L³⁴. Some evidence suggests that schwertmannite formation is thermodynamically more favourable than ferrihydrite between pH 2 and 8, even in solutions containing with low sulphate concentration³⁵. Schwertmannite is a metastable mineral phase and has been observed to transform to goethite, jarosite and hematite over timescales of weeks to months^{34,36,37}.

Poorly crystalline ferrihydrite (amorphous $\text{Fe}(\text{OH})_3$) was most likely the main mineral phase controlling Fe solubility in infiltration rig effluents, with the potential for formation of a more crystalline Fe mineral such as hematite or schwertmannite with time. Study has shown that crystallisation of iron oxyhydroxide precipitates can occur rapidly, within a few hours, in solutions containing high concentrations of iron (i.e. 10^{-2} M Fe^{2+} , or 0.56 mg/L) but may require thousands of years in waters containing dilute concentrations of iron (i.e. 10^{-6} M Fe^{2+} , or 0,056 $\mu\text{g/L}$)³³.

4.3.3 Manganese Minerals

More than 30 unique manganese oxide/hydroxide minerals have been identified across a wide range of geological settings. Manganese minerals are ubiquitous in natural environments and typically found as intermixed, fine-grained, poorly-crystalline aggregates and coatings or in mixtures with iron minerals. Manganese is typically mobile in the acid, organic soils of temperate and subarctic zones, but more likely to concentrate with residual laterites in more alkaline and tropical environments³⁸. Even when present only in trace quantities, manganese minerals can play a significant role in pollutant capture due to their high cation adsorption

³⁴ Bigham, J.M. et al. 1996. Schwertmannite and the chemical modelling of iron in acid sulphate waters. *Geochim. Cosmochim. Acta* 60:2111-2121.

³⁵ Majzlan, J. et al. 2004. Thermodynamics of iron oxides: Part III. Enthalpies of formation and stability of ferrihydrite, schwertmannites and $\epsilon\text{-Fe}_2\text{O}_3$. *Geochim. Cosmochim. Acta* 68:1049-1059.

³⁶ Acero, P. et al. 2006. The behaviour of trace elements during schwertmannite precipitation and subsequent transformation into goethite and jarosite. *Geochim. Cosmochim. Acta* 70:4130–4139.

³⁷ Davidson, L.E. et al. 2008. The kinetics and mechanisms of schwertmannite transformation to goethite and hematite under alkaline conditions. *Am. Mineral.* 93:1326–1337.

³⁸ Post, J.E. 1999. Manganese oxide minerals: crystal structures and economic and environmental significance. *P. Natl. Acad. Sci. USA* 96:3447–3454.

capacities and tendency to scavenge metals and other trace elements in soils and sediments, thereby controlling pollutant lability.

Saturation indices were modelled for a range of different manganese oxide and (oxy)hydroxide minerals to evaluate their potential formation and role in pollutant attenuation in the meso-scale stormwater infiltration study. These included: manganese oxide minerals with a tunnel crystal structure such as pyrolusite ($\beta\text{-MnO}_2$), manganite ($\gamma\text{-MnOOH}$), and nsutite ($\text{Mn}^{4+}_{1-x}\text{Mn}^{2+}_x\text{O}_{2-2x}(\text{OH})_{2x}$); the spinel-like manganese mineral hausmannite ($\text{Mn}^{2+}\text{Mn}^{4+}_2\text{O}_4$); the layered manganese mineral birnessite (variable, e.g. $\text{Na}_{0.5}\text{Mn}_2\text{O}_4 \cdot 1.5\text{H}_2\text{O}$); and numerous manganese phosphate, sulphate and carbonate minerals. Modelling of effluents showed that all manganese minerals were theoretically undersaturated, indicating that in situ manganese mineral formation in the meso-scale stormwater filter was unlikely to have occurred. Examples of modelled manganese mineral saturation indices are shown in Figure 27.

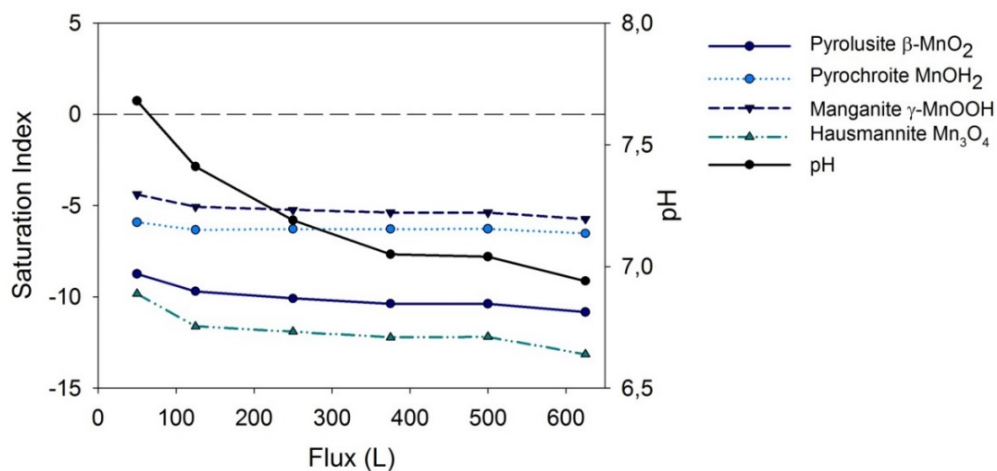


Figure 27. Change in saturation indices (SI) of major manganese mineral phases in infiltration rig meso-scale stormwater filter with increasing stormwater influent flux.

4.3.4 Carbonate Minerals

Carbonate minerals are frequently used to capture trace elements from solution, either through sorption reactions or by incorporation of trace elements into the calcite crystal lattice³⁹. Calcite (CaCO_3) which forms in materials that contain an excess of CaO can sequester trace elements. Within the $\text{MgO-CO}_2\text{-H}_2\text{O}$ system a number of metastable hydrated and basic carbonates can be formed. The stable phases which may form that are in equilibrium with aqueous solutions containing dissolved magnesium and $\text{CO}_{2(g)}$ are either brucite ($\text{Mg}(\text{OH})_2$) or magnesite (MgCO_3)⁴⁰.

Of the basic carbonate minerals modelled, only calcite approached saturation (Figure 28). All other carbonate minerals remained undersaturated throughout the meso-scale stormwater infiltration study. Although modelling showed that dolomite ($\text{CaMg}(\text{CO}_3)_2$) was theoretically approaching saturation in effluents from the infiltration rig, the rate constant of dolomite crystallization at 25 °C is four orders of magnitude lower than that for calcite⁴¹. Thus, calcite was likely the mineral phase controlling Ca concentrations in effluents from the infiltration rig, and potentially sequestering metals via incorporation into the calcite crystal structure as trace impurities.

³⁹ Rimstidt, J.D. et al. 1998. Distribution of trace elements between carbonate minerals and aqueous solutions. *Geochim. Cosmochim. Acta* 62:1851–1863.

⁴⁰ Hänchen, M. et al. 2008. Precipitation in the Mg-carbonate system – effects of temperature and CO_2 pressure. *Chem. Eng. Sci.* 63:1012–1028.

⁴¹ Saldi G.D. et al. 2009. Magnesite growth rates as a function of temperature and saturation state. *Geochim. Cosmochim. Acta* 73:5646–57.

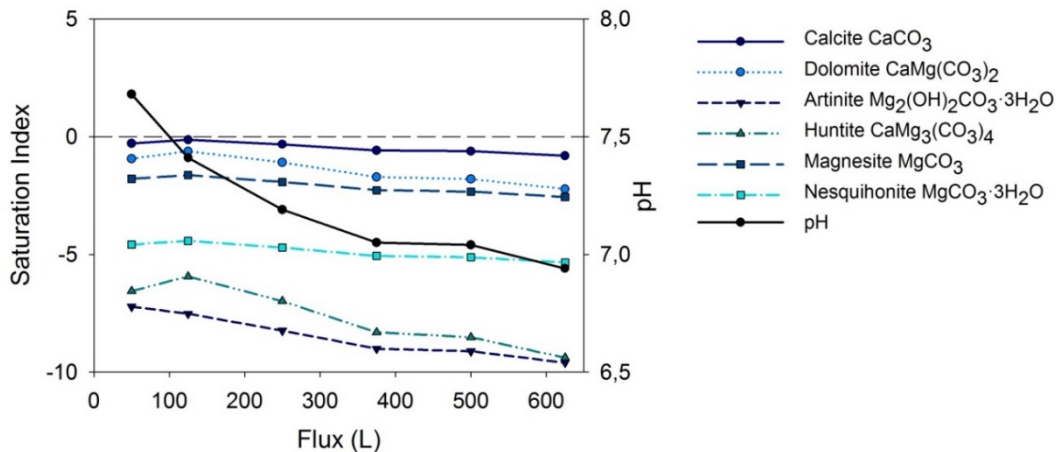


Figure 28. Change in saturation indices (SI) of major carbonate mineral phases in infiltration rig meso-scale stormwater filter with increasing stormwater influent flux.

4.3.5 Sulphate Minerals

Although geochemical modelling indicated thermodynamically favourable conditions for alunite (KAl_3SO_4) precipitation (Figure 29), alunite is stable in solutions of pH 4–7³⁰. Thus, it is unlikely that any of the sulphate minerals shown here (Figure 29) precipitated from solution within the meso-scale stormwater filter. Sulphate concentration was most likely controlled by the aluminium minerals alunite ($KAl_3(SO_4)_2(OH)_6$) or basaluminite ($Al_4SO_4(OH)_{10}\cdot 5H_2O$) (Figure 24), or the iron mineral schwertmannite ($Fe_8O_8(OH)_6(SO_4)_nH_2O$) (Figure 25).

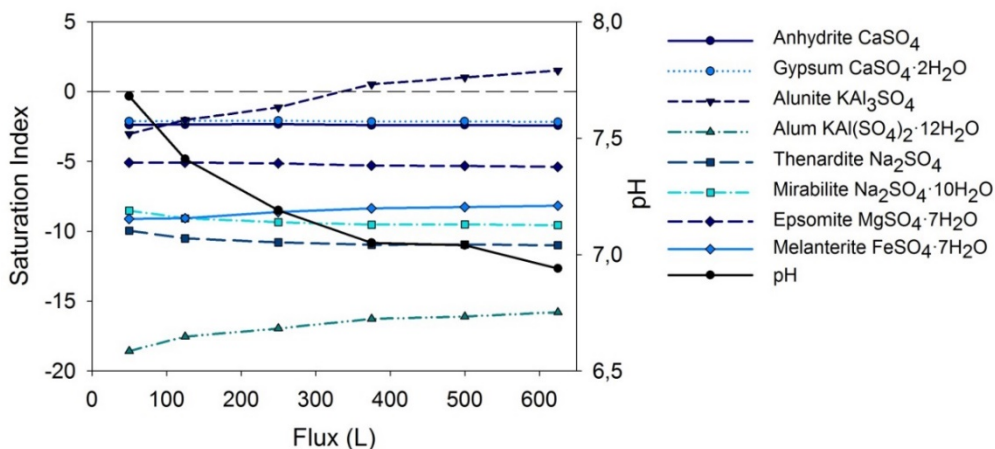


Figure 29. Change in saturation indices (SI) of major sulphate mineral phases in infiltration rig meso-scale stormwater filter with increasing stormwater influent flux.

4.3.6 Phosphate Minerals

Geochemical modelling of numerous phosphate mineral phases showed that hydroxyapatite ($Ca_{10}(PO_4)_6(OH)_2$) was theoretically oversaturated with respect to solution (Figure 30). Hydroxyapatite precipitation becomes kinetically more feasible as solution pH increases, with evidence for hydroxyapatite formation within 24 hours at pH 10–11 at 25 °C⁴². At lower solution pH 7.4–8.4, similar to that of the infiltration rig effluent, hydroxyapatite is most likely to co-precipitate on mineral surfaces⁴³.

⁴² Liu, C. et al. 2001. Kinetics of hydroxyapatite precipitation at pH 10 to 11. *Biomaterials* 22(4):301–306.

⁴³ Inskip, W.P., Silvertooth, J.C. 1988. Kinetics of hydroxyapatite precipitation at pH 7.4 to 8.4. *Geochim. Cosmochim. Acta* 52:1883–1893.

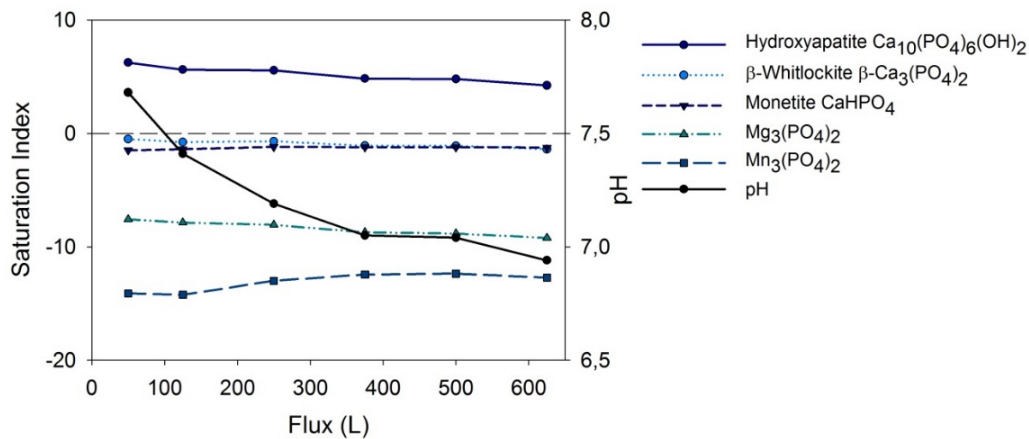


Figure 30. Change in saturation indices (SI) of major phosphate mineral phases in infiltration rig meso-scale stormwater filter with increasing stormwater influent flux.

4.3.7 Copper Minerals

Despite its well-documented strong association with organic matter, copper is known to form mineral precipitates in alkaline environments. Copper hydroxide ($Cu(OH)_2$) typically dominates under neutral to alkaline conditions but according to geochemical modelling was theoretically undersaturated in effluents from the meso-scale stormwater filter (data not shown). Theoretically oversaturated copper minerals included cupric ferrite ($CuFe_2O_4$) and cuprous ferrite ($CuFeO_2$) (Figure 31). Modelling of effluents also showed that the minerals tenorite (CuO) and malachite ($Cu_2(OH)_2CO_3$) were in approximate equilibrium with solution, and thus could also potentially be important mineral phases controlling copper solubility.

Cupric ferrite is the least soluble copper mineral phase⁴⁴. Under oxygen-deficient conditions, reduced iron (Fe^{2+}) can rapidly reduce Cu^{2+} to Cu^{1+} , with the identity of the mineral precipitates formed strongly influenced by chloride concentration⁴⁵. Further, cuprous ferrite ($Cu_2Fe_2O_4$) has been shown to form as a stable mineral phase in waterlogged soil. Thus, formation of both cupric and cuprous ferrite end-members are theoretically possible, assuming cuprous that ferrite formation is limited to poorly oxygenated microsites within the filter matrix. The concentration of copper in solution strongly affects its speciation and behaviour in soil solution or under analogous conditions where copper ions come into contact with solid (mineral) surfaces. Specific adsorption mechanisms are believed to control the activity of copper in solution where concentrations are low¹⁴.

In the modelled stormwater filter system, copper concentration was most likely controlled through a combination of complexation with organic functional groups in the peat substrate, surface adsorption to iron- and/or manganese-hydroxyl functional groups and (co)precipitation reactions with iron and/or manganese oxide minerals.

⁴⁴ Lindsay, W. L. 1979. Chemical equilibria in soils. John Wiley and Sons, New York.

⁴⁵ Matocha, C.J. et al. 2005. Reduction of copper(II) by iron (II). J. Environ. Qual. 34(5):1539–1546.

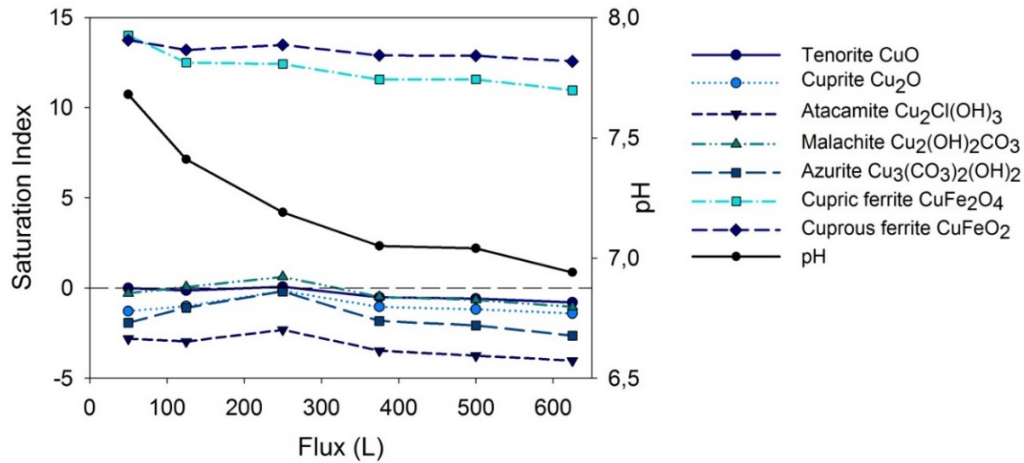


Figure 31. Change in saturation indices (SI) of major copper mineral phases in infiltration rig meso-scale stormwater filter with increasing stormwater influent flux.

4.3.8 Lead Minerals

Similar to copper, lead is known to strongly associate with organic matter and iron oxides and lead solubility is greatest at low pH. Lead is increasingly likely to form insoluble complexes with organic matter, oxide minerals or clay minerals, or to precipitate as lead carbonate, sulphate or phosphate as solution pH increases. Lead phosphate minerals are the least soluble lead minerals in well-oxygenated (aerobic) environments⁴⁶, consistent with the modelled thermodynamic oversaturation of lead phosphate minerals pyromorphite ($\text{Pb}_5(\text{PO}_4)_3\text{Cl}$), plumbgummite ($\text{PbAl}_3(\text{PO}_4)_2\text{OH}_5 \cdot \text{H}_2\text{O}$), hydroxypyromorphite ($\text{Pb}_5(\text{PO}_4)_3\text{OH}$) and lead phosphate ($\text{Pb}_3(\text{PO}_4)_2$) (Figure 32). Geochemical modelling also indicated that cerussite (PbCO_3) was in approximate equilibrium with aqueous effluents throughout the meso-scale stormwater filtration study.

In the present study, lead concentration in infiltration rig effluents was likely controlled by a combination of complexation with organic functional groups in the peat substrate, surface complexation with reactive iron, aluminium and manganese hydroxyl functional groups and (co)precipitation as lead phosphate, or to a lesser extent lead carbonate, mineral phases.

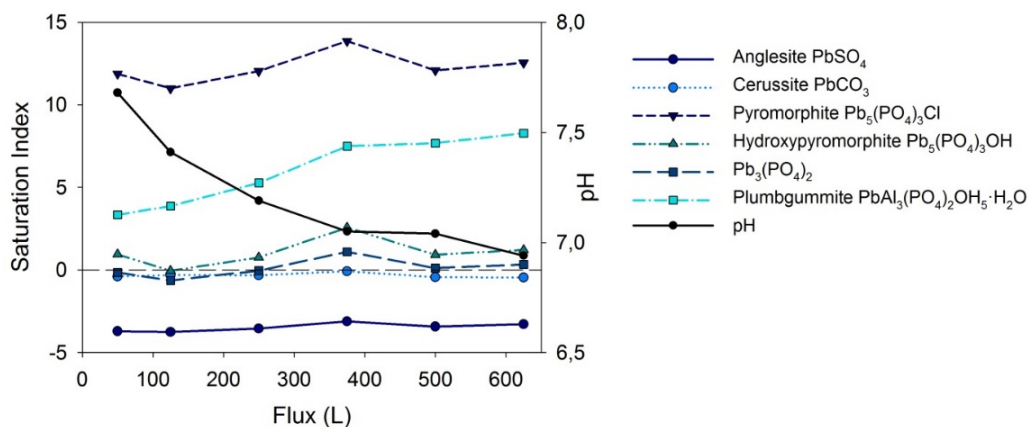


Figure 32. Change in saturation indices (SI) of major lead mineral phases in infiltration rig meso-scale stormwater filter with increasing stormwater influent flux.

⁴⁶ Ma, Q.Y. et al. 1993. In situ lead immobilization by apatite. Environ. Sci. Technol. 27(9):1803–1810.

4.3.9 Zinc Minerals

In natural environments such as soils, zinc solubility is nearly always controlled by sorption reactions with oxyhydroxide minerals and organic matter, as well as clay minerals at high zinc solution concentration^{22,47}. This is reflected in the paucity of zinc mineral phases theoretically oversaturated in meso-scale stormwater filter effluents according to geochemical modelling (Figure 33). Only zinc phosphate ($Zn_3(PO_4)_2 \cdot 4H_2O$) was transiently oversaturated in infiltration rig effluents. Previous work has shown that zinc in soil solution can form low-solubility zinc phosphate precipitates upon addition of a phosphate source⁴⁸. Zinc phosphate mineral precipitates are characterised by low solubility and high resistance to acidification.

The likely fate of zinc in the present study is similar to that of lead. The concentration of zinc in meso-scale stormwater filter effluents was most likely controlled by a combination of surface complexation with reactive iron, aluminium and manganese hydroxyl surface functional groups, complexation with organic functional groups in peat substrate, and by (co)precipitation as zinc phosphate.

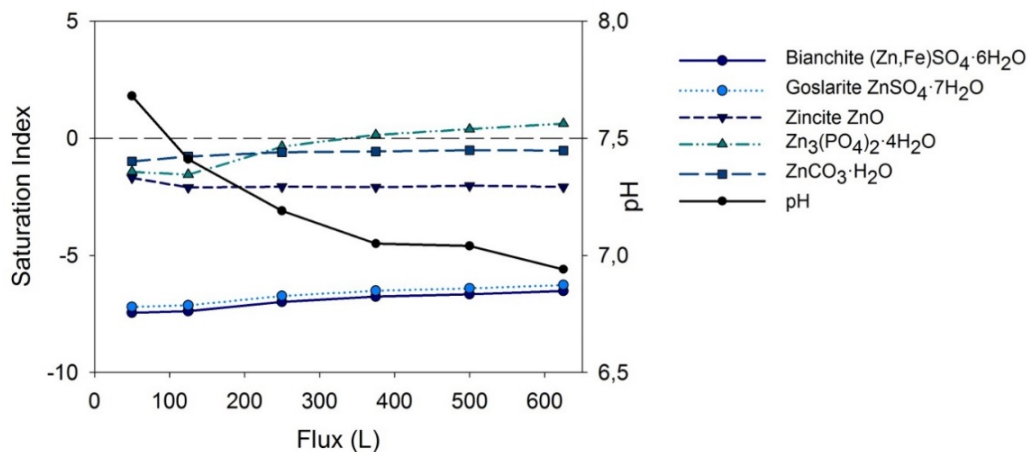


Figure 33. Change in saturation indices (SI) of major zinc mineral phases in infiltration rig meso-scale stormwater filter with increasing stormwater influent flux.

Lead and some copper and zinc in influent stormwater were likely removed through both physical (trapping) and chemical (sorption and/or precipitation) mechanisms. In addition to complexation with organic functional groups on the peat filter material, lead and copper were most likely removed from solution via a combination of complexation with reactive iron, aluminium and manganese hydroxyl surface functional groups and (co)precipitation as metal phosphate, or to a lesser extent carbonate, mineral phases. Similarly, modelling indicated that retention of copper most likely occurred through a combination of surface adsorption to iron- and/or manganese-hydroxyl functional groups and (co)precipitation reactions with iron and/or manganese oxide minerals. Cation exchange and complexation with organic ligands likely also contributed to zinc removal from influent stormwater.

Mechanisms of pollutant attenuation elucidated by geochemical modelling confirm that solution pH is the most significant environmental parameter affecting the behaviour of metals and phosphorus in the stormwater filter systems examined, as the pH affects both ion-solution and mineral surface chemistry.

⁴⁷ Brümmer, G. et al. 1983. Adsorption-desorption and/or precipitation-dissolution processes of zinc in soils. *Geoderma* 31(4):337–354.

⁴⁸ McGowen, S.L. et al. 2001. Use of diammonium phosphate to reduce heavy metal solubility and transport in smelter-contaminated soil. *J. Env. Qual.* 30(2):493–500.

5. Discussion

5.1 Pollutant removal mechanisms

All of the layered or mixed filter material systems examined effectively removed metals (copper, lead and zinc) and phosphorus from stormwater (Table 3, Table 4). Treatment of spruce biochar and 3–8 mm crushed Leca[®] with iron substantially improved phosphorus, and to a lesser extent zinc, retention by layered filter materials (Figure 8, Figure 9). The rates of copper, lead and zinc removal on a mass basis (e.g. g/kg) obtained in these experiments were superior to or comparable with metal adsorption capacities of modified natural materials as reported in the scientific literature^{49,50,51,52}.

The availability of iron, manganese, and aluminium oxide minerals/(oxy)hydroxide surface functional groups was particularly important with respect to zinc retention by filter media. The Leca[®]-peat layered system retained approximately the same quantity of zinc as the Leca[®]-peat-biochar system, and substantially more zinc than the Leca[®]-biochar system. This is consistent with conclusions from geochemical modelling of the meso-scale filter system which indicated that zinc was most likely retained within filter media predominantly via complexation with reactive iron, aluminium and manganese hydroxyl surface functional groups and precipitation as zinc phosphate. Zinc can also be expected to associate with clay mineral surfaces via cation exchange and to form complexes with organic matter (peat). Although the inorganic fraction of peat typically accounts for only a small fraction of its total mass, study has shown that peat in Finland contains on average 6700 mg iron, 2100 mg aluminium, 80 mg manganese, and 4100 mg Ca per kilogram dry material⁵³.

In contrast, phosphorus removal from influent stormwater was also strongly affected by the content of available calcium in filter materials. The increase in phosphorus attenuation following Leca[®] or biochar treatment with iron can be expected based on the well-documented capacity of the formation of strong bonds between phosphate (PO_4^{3-}), the form of phosphorus used in these experiments, and iron oxide/ (oxy)hydroxide mineral surfaces^{12,14,15}. The notably high per cent phosphorus retention by the 10 wt.% biochar-90 wt.% sand mixture, combined with the superior phosphorus retention by Leca[®]-biochar compared with Leca[®]-peat indicates that the formation of calcium phosphate mineral precipitates was a significant mechanism of phosphorus removal. Biochar is known to contain a high proportion of exchangeable calcium and other base cations (i.e. magnesium, potassium)^{24,25,54}. This is supported by results of geochemical modelling which identified the potential for precipitation or co-precipitation of calcium phosphate minerals in the meso-scale filter system containing Leca[®], peat and biochar.

⁴⁹ Barakat, M.A. 2011. New trends in removing heavy metals from industrial wastewater. *Arabian J. Chem.* 4(4):361–377.

⁵⁰ Cucarella, V., Renman, G. 2009. Phosphorus sorption capacity of filter materials used for on-site wastewater treatment determined in batch experiments – A comparative study. *J. Env. Qual.* 38:381–392.

⁵¹ Ho, Y.S., McKay, G. 2000. The kinetics of sorption of divalent metal ions onto sphagnum moss peat. *Water Res.* 34(3):735–742.

⁵² McKenzie, R.M. 1980. The adsorption of lead and other heavy metals on oxides of manganese and iron. *Aust. J. Soil Res.* 18:61–73.

⁵³ Guan, T. 2015. An overview of peat related chemistry. Centria University of Applied Sciences, Ylivieska, Finland.

⁵⁴ Singh et al. 2010. Characterisation and evaluation of biochars for their application as a soil amendment. *Aus. J. Soil. Res.* 48:516–525.

Table 3. Pollutant removal from stormwater by layered or mixed filter material systems following 37.5 litres of 10X concentrated synthetic stormwater flow through each respective filter system in laboratory column trials. All systems contained layers of KaM 0-5 mm aggregate above and below shown phases. Values representing $\geq 80\%$ pollutant removal are highlighted in blue.

	Cu ²⁺			Pb ²⁺			Zn ²⁺			PO ₄ ³⁻ / P ⁵⁺		
	g/m ³	%	g/m ³	g/m ³	%	g/m ³	g/m ³	%	g/m ³	g/m ³	%	g/m ³
Leca® / Peat / Biochar	28.8	86.4	64.0	88.4	88.4	94.4	70.0	13.3	43.1			
Leca® / Peat / Fe-Biochar	32.5	97.3	70.7	97.6	130	96.2	25.2	81.4				
Fe-Leca® / Peat / Biochar	31.4	94.2	69.1	95.4	106	79.0	18.8	60.9				
Biochar - Sand	31.8	95.4	70.3	97.0	108	80.1	22.0	71.1				
Leca® / Peat	29.2	87.5	63.0	86.9	96.2	71.4	12.8	41.6				
Leca® / Biochar	27.0	80.9	61.0	84.2	67.3	50.0	18.9	60.7				

Table 4. Pollutant removal from stormwater by layered filter material system following 625 litres of 10X concentrated synthetic stormwater flow through the meso-scale stormwater filter system in the infiltration rig study. The materials shown were layered between KaM 0-5 mm aggregate above and below. Values representing $\geq 80\%$ pollutant removal are highlighted in blue.

	Cu ²⁺			Pb ²⁺			Zn ²⁺			PO ₄ ³⁻ / P ⁵⁺		
	g/m ³	%	g/m ³	g/m ³	%	g/m ³	g/m ³	%	g/m ³	g/m ³	%	
Leca® / Peat / Biochar	10.7	97.4	26.7	99.7	39.4	87.1	8.42	80.7				

Lead and some copper in influent stormwater were likely removed through both physical (trapping) and chemical (sorption and/or precipitation) mechanisms. Previous work has demonstrated that lead in urban runoff is largely particulate-associated and rarely present in dissolved form, whereas copper is typically present in both dissolved and particulate form and zinc is usually dissolved⁵⁵. For this reason, filter material porosity and pore size distribution, and the tortuosity of the infiltration pathway are significant parameters with respect to the retention of particulate-associated pollutants.

The aggregate (KaM 0/5) material¹⁰ used in the present experiments as a low-hydraulic conductivity layer to slow stormwater movement through filter media and the 0–2 mm quartz sand mixed with biochar in the biochar-sand filter would both serve to effectively increase the tortuosity of the infiltration pathway by virtue of the small particle size and closer particle packing density relative to other materials, thus enhancing retention of particulate-associated pollutants. The aggregate also likely contributed to some extent to dissolved pollutant removal through mineral surface interactions, as the KaM 0/5 aggregate was granite-based and comprised of numerous primary minerals in addition to quartz (e.g. orthoclase and plagioclase feldspars, biotite and muscovite micas, and carbonates).

Similarly, modelling indicated that retention of the slightly more soluble pollutant copper most likely occurred through a combination of surface adsorption to iron- and/or manganese-hydroxyl functional groups and (co)precipitation reactions with iron and/or manganese oxide minerals. This is consistent with the observed copper retention by different filter systems (Figure 6) in the column trial, as well as by results of the meso-scale stormwater filtration experiment. Specific adsorption of copper, lead and zinc to organic and hydrous oxide functional groups is known to occur in the preferential order: lead > copper > zinc⁵⁶, which is also consistent with results of geochemical modelling and results of experiments outlined herein. The retention of copper, as well as other metals and phosphorus by the Leca[®] filter material likely occurred primarily via interaction with aluminium (oxy)hydroxide surface functional groups^{23,57,58}.

5.2 Implications for implementation

None of the layered or mixed stormwater filter systems reached capacity for copper, lead, zinc or phosphorus removal during the experiments described herein. Geochemical modelling of effluents from the meso-scale stormwater filter comprised of layered 3–8 mm crushed Leca[®]/peat with 10 wt.% limestone/ spruce biochar indicated that a combination of surface (ad)sorption and (co)precipitation reactions likely contributed to metal and phosphorus removal from stormwater within the filter system.

The identified mechanisms of phosphorus removal – specific sorption of phosphate to iron oxide/ (oxy)hydroxide mineral surfaces and the formation of calcium phosphate mineral precipitates – indicate that in the absence of significant changes in pH or oxidation-reduction potential, the removed phosphorus is strongly retained and unlikely to be re-mobilised. Phosphate specifically adsorbed to iron oxide/(oxy)hydroxide minerals has very limited biological availability, whilst phosphorus in precipitated calcium phosphate minerals is only slowly available for biological uptake through physical and chemical weathering processes. The specificity of lead and copper sorption to organic and hydrous oxide functional groups coupled with the formation of very low-solubility lead phosphate minerals implies reasonable long-term stability of retained lead and copper within filter materials, assuming no significant

⁵⁵ Tuccillo, M.E: 2006. Size fractionation of metals in runoff from residential and highway storm sewers. *Sci. Total Environ.* 355:288–300.

⁵⁶ Alloway, B.J. 1995. Soil processes and the behaviour of metals. In: B.J. Alloway (ed.) *Heavy Metals in Soils*, Blackie, Glasgow.

⁵⁷ Zhu, T: et al. 1997. Phosphorus sorption and chemical characteristics of lightweight aggregates (LWA) – potential filter media in treatment wetlands. *Water Sci. Technol.* 35(5):103–108.

⁵⁸ McBride, M.B. 1982. Cu²⁺-adsorption characteristics of aluminum hydroxide and oxyhydroxides. *Clays Clay Miner.* 30(1):21–28.

changes in pH or oxidation-reduction potential. Similarly, zinc immobilised within metal phosphate precipitates would be expected to be stable in the longer term.

Of the metals investigated herein, zinc adsorbed to mineral surfaces or complexed with organic matter is the most likely to be out-competed by other cations for sorption sites. Thus its retention on filter materials is the least stable in the longer term. Release of retained zinc from filter materials would be an indication that the filter's capacity for stormwater purification has been exceeded and needs to be renewed. Prior to zinc release, however, declining rates of zinc retention would indicate that the filter materials were approaching the end of their functional lifespan.

Each of the laboratory-scale columns treated a total of 37.5 L synthetic stormwater. The tested stormwater influent volume was equivalent to >65 000 L normal 1X concentrated stormwater runoff per cubic metre of 'reactive' filter material, or nearly 60 000 L stormwater runoff per cubic metre of each filter system including upper and lower coarse aggregate layers. These results suggest that all filter systems examined could effectively attenuate copper, lead, zinc and phosphorus in stormwater runoff in the mid- to longer term (e.g. 5–10 years or more depending on dimensioning of the stormwater filtration system), consistent with results of previous work using individual filter materials¹⁰.

Up-scaling from 0.006 m³ layered filter systems within laboratory columns to a 0.3 m³ layered filter system within the meso-scale infiltration rig clearly showed the effects of increased solid-to-solution ratio (increased adsorbent area) on contaminant attenuation. Experiments using smaller-scale laboratory columns delivered 1.5 L aliquots of synthetic stormwater to a ca. 0.006 m³ volume of layered KaM 0-5 mm aggregate + 3–8 mm crushed Leca[®]/ peat with 10 wt.% limestone/ spruce biochar filter materials; 25 L aliquots of synthetic stormwater were delivered to a 0.3 m³ volume of layered aggregate + Leca[®]-peat-biochar in the infiltration rig experiment. The ratio of filter material volume to influent stormwater volume was approximately three times greater in the meso-scale study compared with the smaller-scale laboratory column experiment.

The relative increase in filter volume/ mass with respect to the volume of influent stormwater in the meso-scale study clearly showed enhanced pollutant removal efficiency. The quantity of stormwater filtered through the meso-scale layered system was equivalent to nearly 21 000 L of normal 1X concentrated stormwater runoff per cubic metre of 'reactive' filter material, or nearly 7 000 L stormwater runoff per cubic metre of the filter system including upper and lower coarse aggregate layers. Results of the meso-scale study suggest that a lesser rate of stormwater loading can increase contaminant removal efficiency. The observed difference in pollutant retention efficiency between these two analogous Leca[®]/peat/biochar filter systems examined herein suggests that a greater volume/ mass of filter material will provide more effective treatment of stormwater runoff. This highlights the importance of hydraulic modelling and load estimation for the scaling of filter systems not only for flood control, but also for stormwater quality improvement.

6. Conclusions

Reactive filter material use in engineered stormwater management systems can provide substantial water quality benefits in passive and semi-passive stormwater treatment structures, and can provide fit-for-purpose treatment options for on-site runoff quality management. The results of the present study provide essential knowledge about the use of reactive filter media for stormwater treatment, facilitating the use of engineered infiltration or subsurface filtration media to manage not only stormwater quantity but also stormwater quality.

Decentralized engineered water management structures are increasingly being used in urban areas to trap, infiltrate and/or harvest stormwater. Green infrastructure systems including rain gardens, green roofs, permeable pavements, swales, wetlands and others can benefit from

the use of appropriate reactive filter materials to enhance both pollutant removal capacity and efficiency. All of the filtration systems examined herein showed strong potential for use to remove metals and phosphorus from stormwater runoff. Although it was not possible to conclusively estimate individual contaminant capacities for each of the respective filter materials, results indicate a likely effective lifespan in the range of up to ca. 10 years in the absence of physical clogging or similar malfunctions, and depending upon infiltration structure design and scale.

Results of the present study in combination with previous work¹⁰ show that engineered stormwater infiltration systems containing individual filter materials or select combinations of reactive filter media can improve stormwater runoff quality. Pollutant removal from runoff prior to water infiltration, uptake by collection systems or discharge to receiving waterbodies will reduce pollutant loads to aquatic environments. In addition, purification of stormwater runoff facilitates its potential use as an alternative non-potable water supply thereby reducing pressure on over-exploited water resources and contributing to long-term water resource sustainability.

Appendix I. Results of column tests using layered filtration media

Table 5 shows the raw data obtained from laboratory column experiments using filter materials in layered configuration or as a mixture (between layers of aggregate; Figure 3). The synthetic stormwater used contained 10X a 'normal' concentration of phosphorus, copper, lead and zinc (Table 1). Column effluents were analysed using inductively-coupled plasma spectrophotometry – atomic emission spectroscopy (ICP-AES) or ICP-mass spectrometry (ICP-MS).

Table 5. Composition of influent synthetic stormwater and effluents from laboratory columns containing filter materials in layered configuration or as a homogeneous mixture (e.g. biochar and sand).

Material	Cumulative flux (L)	pH	Concentration (µg/l)			
			P	Cu	Pb	Zn
Influent stormwater	3	6.40	5000	5400	13000	21000
	7.5	6.15	5600	6800	17000	21000
	15	6.14	4800	5000	11000	20000
	22.5	6.17	4100	3900	5700	20000
	30	6.18	4400	4800	9700	20000
	37.5	6.22	4400	4900	12000	22000
Leca® / Peat + 10 wt.% limestone / Spruce biochar (L-P-B)	3	7.59	2400	1100	2200	6400
	7.5	7.23	2600	1100	2100	5900
	15	6.90	2800	610	1200	5500
	22.5	7.00	2700	400	540	5600
	30	6.74	2800	480	870	7000
	37.5	7.06	2600	620	1100	6900
Leca® / Peat + 10 wt.% limestone / Fe-biochar L-P-FeB	3	8.95	350	150	280	790
	7.5	9.54	870	120	220	660
	15	9.44	1100	160	380	730
	22.5	9.42	930	130	250	830
	30	9.22	910	120	200	850
	37.5	9.19	950	140	270	820
Fe-Leca® / Peat + 10 wt.% limestone / Spruce biochar FeL-P-B	3	8.10	1400	510	840	3300
	7.5	7.49	1500	470	830	2800
	15	7.08	2000	230	530	3700
	22.5	7.16	1900	240	290	4700
	30	6.86	2100	180	280	5800
	37.5	7.18	2000	180	420	5500
10 wt.% Spruce biochar-90 wt.% Sand 10B-90S	3	8.12	870	450	770	2900
	7.5	7.81	1100	350	610	2500
	15	7.54	1500	220	380	2700
	22.5	7.48	1400	120	88	3500
	30	7.17	1700	160	120	7200
	37.5	7.27	1400	130	100	5900
Leca® / Peat + 10 wt.% limestone L-P	3	7.24	2500	800	2000	4500
	7.5	6.72	2900	1100	2600	5600
	15	6.64	2900	700	1600	6000
	22.5	6.63	2700	330	510	5500
	30	6.45	2700	430	1000	6500
	37.5	6.61	2700	540	1300	7400
Leca® / Spruce biochar L-B	3	7.89	1700	990	2100	5900
	7.5	7.61	980	350	790	3400
	15	7.01	1900	940	1600	10000
	22.5	7.06	1700	630	1100	12000
	30	6.72	2500	1600	2700	15000
	37.5	6.83	2300	1400	2400	15000

Appendix II. Results of meso-scale study using layered filtration media

Table 6 shows the raw data obtained from the meso-scale infiltration rig study using 3–8 mm crushed Leca[®] / peat + 10 wt.% limestone / spruce biochar filter materials in layered configuration (Figure 20). The synthetic stormwater used contained 10X a ‘normal’ concentration of phosphorus, copper, lead and zinc (Table 1). Column effluents were analysed using inductively-coupled plasma spectrophotometry – atomic emission spectroscopy (ICP-AES) or ICP-mass spectrometry (ICP-MS).

Table 6. Composition of influent synthetic stormwater and effluents from meso-scale stormwater filter (infiltration rig) containing layered 3–8 mm crushed Leca® / peat + 10 wt.% limestone / spruce biochar.

	Cumulative flux (L)	pH	EC (µS/cm)	P (mg/L)	Cu (mg/L)	Pb (mg/L)	Zn (mg/L)	SO ₄ ²⁻ (mg/L)	Cl ⁻ (mg/L)
Influent stormwater	50	6.00	526	4.80	5.20	12.0	20.0	ND	ND
	125	6.64	266	4.90	5.20	13.0	20.0	ND	ND
	250	6.13	266	4.90	5.20	13.0	21.0	ND	ND
	375	6.04	259	4.80	5.10	13.0	23.0	ND	ND
	500	5.99	260	5.10	5.10	13.0	23.0	ND	ND
	625	6.03	259	5.90	6.20	13.0	23.0	ND	ND
Effluent from filter system	50	7.68	456	0.47	0.03	0.03	0.21	47.0	36.0
	125	7.41	532	0.58	0.08	0.03	0.30	43.0	25.0
	250	7.19	466	0.89	0.18	0.04	0.83	37.0	26.0
	375	7.05	384	1.00	0.06	0.08	1.40	33.0	19.0
	500	7.04	351	1.00	0.05	0.04	1.70	34.0	14.0
	625	6.94	328	1.10	0.04	0.04	2.30	33.0	16.0

Table 6 (continued). Composition of influent synthetic stormwater and effluents from meso-scale stormwater filter (infiltration rig) containing layered 3–8 mm crushed Leca® / peat + 10 wt. % limestone / spruce biochar.

	TOC (mg/L)	TIC (mg/L)	Al (mg/L)	Ca (mg/L)	Fe (mg/L)	Mg (mg/L)	Mn (mg/L)	K (mg/L)	Na (mg/L)	Si (mg/L)
Influent stormwater	ND	ND	ND	ND	ND	ND	ND	ND	ND	ND
	ND	ND	ND	ND	ND	ND	ND	ND	ND	ND
	ND	ND	ND	ND	ND	ND	ND	ND	ND	ND
	ND	ND	ND	ND	ND	ND	ND	ND	ND	ND
	ND	ND	ND	ND	ND	ND	ND	ND	ND	ND
	ND	ND	ND	ND	ND	ND	ND	ND	ND	ND
Effluent from filter system	5,60	22,00	0,13	33,00	0,07	6,50	0,07	18,00	21,00	5,70
	18,00	43,00	0,07	42,00	0,03	8,10	0,10	42,00	12,00	6,60
	14,00	33,00	0,06	52,00	0,03	8,20	0,29	34,00	9,50	8,50
	9,10	27,00	0,14	46,00	0,04	5,90	0,52	24,00	8,00	8,40
	7,90	29,00	0,20	46,00	0,04	5,50	0,56	21,00	8,10	9,20
7,20	27,00	0,20	42,00	0,04	4,70	0,49	18,00	7,60	8,60	

Appendix III. Results of geochemical modelling of effluents from meso-scale study using layered filtration media

Table 7 shows results of geochemical modelling of effluents from the meso-scale infiltration rig study using 3–8 mm crushed Leca[®] / peat + 10 wt.% limestone / spruce biochar filter materials in layered configuration (Figure 20). The synthetic stormwater used contained 10X the ‘normal’ stormwater concentration of phosphorus, copper, lead and zinc¹⁰ (Table 1). PHREEQC Interactive Version 3.3.3⁵⁹ was used to model the hydro-geochemistry of major ions Na⁺, K⁺, Ca²⁺, Mg²⁺, Cl⁻, HCO₃⁻, SO₄²⁻ as well as Fe²⁺, Al³⁺, Mn²⁺, P⁵⁺, Cu²⁺, Pb²⁺, and Zn²⁺. Saturation indices (SIs) of mineral phases were estimated using PHREEQC calculations. Model input parameters were sourced from the minteq.v4 database.

⁵⁹ Parkhurst, D.L., Appelo, C.A.J. 2013. Description of input and examples for PHREEQC version 3 - A computer program for speciation, batch-reaction, one-dimensional transport, and inverse geochemical calculations. United States Department of the Interior, Washington, DC.

Table 7. Saturation indices (SIs) of selected mineral phases present in effluents from the meso-scale infiltration rig study using layered 3-8 mm crushed Leca® / peat + 10 wt.% limestone / spruce biochar.

Flux (L)	Alunite	Anglesite	Anhydrite	Antlerite	Aragonite	Artinite	Atacamite	Azurite	Basaluminitite
	$KAl_3(SO_4)_2(OH)_6$	$PbSO_4$	$CaSO_4$	$Cu_3(SO_4)(OH)_4$	$CaCO_3$	$Mg_2(OH)_2CO_3 \cdot 3H_2O$	$Cu_2Cl(OH)_3$	$Cu_3(CO_3)_2(OH)_2$	$Al_4(OH)_{10}SO_4$
50	-3.04	-3.70	-2.38	-4.70	-0.47	-7.22	-2.81	-1.93	-2.95
125	-2.04	-3.75	-2.36	-4.62	-0.31	-7.53	-2.96	-1.09	-2.53
250	-1.14	-3.55	-2.34	-3.65	-0.51	-8.24	-2.32	-0.19	-1.52
375	0.52	-3.12	-2.41	-5.15	-0.77	-9.01	-3.48	-1.82	0.66
500	1.01	-3.42	-2.39	-5.34	-0.80	-9.12	-3.75	-2.08	1.35
625	1.50	-3.29	-2.43	-5.79	-0.99	-9.60	-4.02	-2.64	1.89
Flux (L)	Bianchite	Bimessite	Bixbyite	Boehmite	Brochantite	Brucite	β -Whitlockite	Octocalcium phosphate	Monetite
	$(Zn,FeSO_4) \cdot 6H_2O$	MnO_2	Mn_2O_3	$AlOOH$	$Cu_4SO_4(OH)_6$	$Mg(OH)_2$	$\beta-Ca_3(PO_4)_2$	$Ca_4H(PO_4)_3 \cdot 3H_2O$	$CaHPO_4$
50	-7.45	-10.80	-8.14	1.07	-3.49	-4.67	-0.51	-3.12	-1.50
125	-7.38	-11.76	-9.51	1.06	-3.55	-5.13	-0.77	-3.29	-1.40
250	-6.98	-12.15	-9.85	1.22	-2.36	-5.56	-0.71	-3.02	-1.20
375	-6.76	-12.44	-10.15	1.70	-4.45	-5.97	-1.09	-3.43	-1.23
500	-6.66	-12.44	-10.14	1.87	-4.72	-6.02	-1.10	-3.45	-1.23
625	-6.52	-12.89	-10.84	1.95	-5.38	-6.28	-1.40	-3.78	-1.26

Table 7 (continued). Saturation indices (SIs) of selected mineral phases present in effluents from the meso-scale infiltration rig study using layered 3–8 mm crushed Leca® / peat + 10 wt.% limestone / spruce biochar.

Flux (L)	Brushite CaHPO ₄ ·2H ₂ O	Calcite CaCO ₃	Cerussite PbCO ₃	Chalcanthite CuSO ₄ ·5H ₂ O	Chalcedony SiO ₂	Chrysotile Mg ₃ (Si ₂ O ₅)(OH) ₄	Corundum Al ₂ O ₃	Cotunnite PbCl ₂	Cristoballite α-SiO ₂
50	-1.78	-0.29	-0.40	-8.57	-0.15	-4.69	-0.35	-9.27	-0.35
125	-1.68	-0.13	-0.31	-8.22	-0.08	-5.95	-0.38	-9.59	-0.28
250	-1.48	-0.33	-0.33	-7.65	0.03	-7.02	-0.06	-9.28	-0.17
375	-1.51	-0.59	-0.08	-7.99	0.03	-8.26	0.91	-9.07	-0.17
500	-1.51	-0.62	-0.43	-8.03	0.07	-8.33	1.24	-9.66	-0.13
625	-1.54	-0.81	-0.46	-8.05	0.04	-9.17	1.41	-9.40	-0.16
Flux (L)	Spertiniite Cu(OH) ₂	Chalcocyanite CuSO ₄	Cupric carbonate CuCO ₃	Cupric ferrite Cu ₃ (PO ₄) ₂ ·3H ₂ O	Cu metal Cu ⁰	Cupric ferrite CuFe ₂ O ₄	Cuprite Cu ₂ O	Cuprous ferrite CuFeO ₂	
50	-1.03	-14.15	-5.98	-7.71	-4.27	14.00	-1.28	13.75	
125	-1.16	-13.80	-5.27	-7.00	-3.86	12.50	-1.01	13.20	
250	-0.96	-13.23	-3.57	-5.30	-3.22	12.41	-0.16	13.48	
375	-1.54	-13.57	-4.74	-6.47	-3.52	11.56	-1.04	12.90	
500	-1.62	-13.61	-4.94	-6.67	-3.58	11.57	-1.18	12.88	
625	-1.83	-13.63	-5.18	-6.91	-3.59	10.96	-1.40	12.56	

Table 7 (continued). Saturation indices (SIs) of selected mineral phases present in effluents from the meso-scale infiltration rig study using layered 3–8 mm crushed Leca® / peat + 10 wt.% limestone / spruce biochar.

Flux (L)	Diaspore AlOOH	Dolomite CaMg(CO ₃) ₂	Epsomite MgSO ₄ ·7H ₂ O	Fe(OH) ₂	Fe(OH) ₂ ·ClO ₃	Mikasaite Fe ₂ (SO ₄) ₃	Ferrihydrite Fe(OH) _{3(am)}	Gibbsite Al(OH) ₃
50	2.78	-0.94	-5.09	-6.04	6.00	-40.48	2.98	1.36
125	2.76	-0.62	-5.08	-6.45	5.35	-40.41	2.30	1.34
250	2.92	-1.10	-5.14	-6.38	5.27	-39.61	2.15	1.51
375	3.41	-1.72	-5.31	-6.38	5.14	-39.14	2.02	1.99
500	3.57	-1.81	-5.32	-6.32	5.15	-38.95	2.06	2.15
625	3.66	-2.23	-5.39	-6.42	5.00	-38.76	1.86	2.24
Flux (L)	Goethite α-FeOOH	Goslarite ZnSO ₄ ·7(H ₂ O)	Greenalite (Fe ²⁺ , Fe ³⁺) ₂ Si ₂ O ₅ (OH) ₄	Gypsum CaSO ₄ ·2H ₂ O	Halite NaCl	Halloysite Al ₂ Si ₂ O ₅ (OH) ₄	Hausmannite Mn ₃ O ₄	Hercynite FeAl ₂ O ₄
50	5.68	-7.20	-5.62	-2.13	-7.70	2.34	-9.84	3.94
125	5.00	-7.14	-6.74	-2.11	-8.11	2.44	-11.62	3.49
250	4.85	-6.74	-6.30	-2.09	-8.19	2.98	-11.91	3.89
375	4.72	-6.51	-6.29	-2.16	-8.40	3.94	-12.22	4.86
500	4.76	-6.41	-6.05	-2.14	-8.53	4.34	-12.19	5.24
625	4.56	-6.27	-6.40	-2.18	-8.49	4.46	-13.14	5.31



Table 7 (continued). Saturation indices (SIs) of selected mineral phases present in effluents from the meso-scale infiltration rig study using layered 3–8 mm crushed Leca® / peat + 10 wt.% limestone / spruce biochar.

Flux (L)	Huntite CaMg ₃ (CO ₃) ₄	Hydrocerussite Pb ₃ (OH) ₂ (CO ₃) ₂	Hydromagnesite Mg ₅ (CO ₃) ₄ (OH) ₂ ·4H ₂ O	Hydrotalcite MgAl Mg ₆ Al ₂ (OH) ₁₆ (OH) ₂	Hydrotalcite MgFe Mg ₆ Fe ₂ (OH) ₁₆ (OH) ₂	Hydroxyapatite Ca ₁₀ (PO ₄) ₆ (OH) ₂	Hydroxy- pyromorphite Pb ₅ (PO ₄) ₃ OH	Jurbanite AlSO ₄ (OH)·5H ₂ O	K-Alum KAl(SO ₄) ₂ ·12(H ₂ O)
50	-6.56	-0.92	-16.61	37.19	30.24	6.25	0.94	-5.97	-18.57
125	-5.94	-1.27	-16.45	34.39	26.10	5.62	-0.05	-5.51	-17.54
250	-6.99	-1.47	-18.02	32.13	23.22	5.55	0.76	-4.98	-16.96
375	-8.31	-0.80	-19.85	30.64	20.49	4.82	2.57	-4.25	-16.27
500	-8.52	-1.84	-20.14	30.67	20.29	4.78	0.92	-4.05	-16.11
625	-9.39	-1.95	-21.30	29.27	18.32	4.22	1.22	-3.77	-15.79
Flux (L)	K-Jarosite KFe ₃ (SO ₄) ₂ (OH) ₆	Na-Jarosite NaFe ₃ (SO ₄) ₂ (OH) ₆	Kaolinite Al ₂ Si ₂ O ₅ (OH) ₄	Langite Cu ₄ (SO ₄)(OH) ₆ ·2H ₂ O	Lamarkite PbSO ₄	Laurionite PbOHCl	Lepidocrocite FeOOH	Lime CaO	Litharge PbO
50	-0.07	-3.38	4.48	-5.76	-3.70	-3.97	4.80	-20.59	-5.33
125	-1.08	-5.00	4.58	-5.81	-4.28	-4.39	4.12	-21.04	-5.86
250	-1.10	-5.02	5.12	-4.63	-4.24	-4.32	3.97	-21.38	-6.03
375	-1.30	-5.15	6.08	-6.71	-3.62	-4.12	3.84	-21.70	-5.84
500	-1.17	-4.95	6.48	-6.99	-4.27	-4.59	3.88	-21.72	-6.18
625	-1.54	-5.28	6.60	-7.64	-4.19	-4.49	3.68	-21.95	-6.24



Table 7 (continued). Saturation indices (SIs) of selected mineral phases present in effluents from the meso-scale infiltration rig study using layered 3–8 mm crushed Leca® / peat + 10 wt.% limestone / spruce biochar.

Flux (L)	Maghemite	Magnesioferrite	Magnesite	Magnetite	Malachite	Manganite	Massicot	Melanothallite	Melanterite
	$\gamma\text{-Fe}_2\text{O}_3$	Fe_2MgO_4	MgCO_3	Fe_3O_4	$\text{Cu}_2(\text{OH})_2\text{CO}_3$	MnOOH	PbO	CuCl_2	$\text{FeSO}_4 \cdot 7\text{H}_2\text{O}$
50	5.96	7.12	-1.79	16.47	-0.29	-4.38	-5.53	-20.02	-9.12
125	4.59	5.29	-1.64	14.68	0.06	-5.07	-6.06	-19.94	-9.06
250	4.30	4.57	-1.92	14.47	0.62	-5.24	-6.23	-19.26	-8.62
375	4.03	3.88	-2.28	14.20	-0.49	-5.39	-6.04	-19.83	-8.37
500	4.11	3.92	-2.34	14.34	-0.66	-5.38	-6.38	-20.15	-8.28
625	3.72	3.26	-2.56	13.85	-1.04	-5.73	-6.44	-20.05	-8.18
Flux (L)	Farringtonite	Newberyite	Minium	Mirabilite	Reddingite				
	$\text{Mg}_3(\text{PO}_4)_2$	$\text{MgHPO}_4 \cdot 3\text{H}_2\text{O}$	Pb_3O_4	$\text{Na}_2\text{SO}_4 \cdot 10\text{H}_2\text{O}$	$\text{Mn}_2(\text{SO}_4)_3$	$\text{Mn}_3(\text{PO}_4)_2$	$\text{MnCl}_2 \cdot 4\text{H}_2\text{O}$	MnHPO_4	MnSO_4
50	-7.59	-3.08	-28.08	-8.52	-59.63	-14.11	-14.85	1.80	-12.16
125	-7.87	-2.99	-30.21	-9.08	-59.56	-14.24	-15.05	1.93	-12.09
250	-8.07	-2.87	-31.14	-9.36	-58.81	-13.00	-14.52	2.53	-11.68
375	-8.72	-2.99	-30.86	-9.54	-58.37	-12.45	-14.52	2.81	-11.44
500	-8.84	-3.02	-31.90	-9.51	-58.26	-12.38	-14.75	2.84	-11.39
625	-9.22	-3.09	-32.28	-9.57	-58.37	-12.73	-14.68	2.79	-11.45



Table 7 (continued). Saturation indices (SIs) of selected mineral phases present in effluents from the meso-scale infiltration rig study using layered 3–8 mm crushed Leca® / peat + 10 wt.% limestone / spruce biochar.

Flux (L)	Nantokite	Natron	Nesquehonite	Nsutite	Plumbonacrite	Merreheadite	Pb ₂ O ₃
	CuCl	Na ₂ CO ₃ ·10H ₂ O	MgCO ₃ ·3H ₂ O	MnO ₂			
50	-5.32	-10.36	-4.58	-10.22	-42.95	-11.47	-22.96
125	-5.08	-10.78	-4.43	-11.17	-44.55	-12.53	-24.56
250	-4.41	-11.27	-4.71	-11.56	-45.31	-12.86	-25.33
375	-4.85	-11.64	-5.07	-11.85	-43.10	-12.48	-25.23
500	-5.04	-11.66	-5.13	-11.86	-46.57	-13.16	-25.93
625	-4.99	-11.88	-5.35	-12.31	-46.94	-13.28	-26.25
Shannonite							
Flux (L)	Pb ₂ OCO ₃	Pb ₃ (PO ₄) ₂	Pb ₃ O ₂ CO ₃	Pb ₃ O ₂ SO ₄	Pb ₃ O ₃ SO ₄	Pb metal	PbO·0.3H ₂ O
50	-5.61	-0.15	-9.83	-7.46	-11.29	Pb ⁰	-5.62
125	-6.05	-0.64	-10.80	-8.57	-12.93	PbHPO ₄	-6.15
250	-6.23	-0.04	-11.14	-8.70	-13.22	Pb ⁰	-6.31
375	-5.80	1.10	-10.52	-7.89	-12.23	Pb ⁰	-6.13
500	-6.49	0.11	-11.56	-8.87	-13.55	Pb ⁰	-6.47
625	-6.57	0.33	-11.70	-8.86	-13.59	Pb ⁰	-6.53

Table 7 (continued). Saturation indices (SIs) of selected mineral phases present in effluents from the meso-scale infiltration rig study using layered 3–8 mm crushed Leca® / peat + 10 wt.% limestone / spruce biochar.

Flux (L)	Periclase	Phosgenite	Plattnerite	Plumbgummitte	Portlandite	Pyrochroite	Pyrolusite	Pyromorphite	Quartz
	MgO	PbCl ₂ ·PbCO ₃	PbO ₂	PbAl ₃ (PO ₄) ₂ (OH) ₅ ·H ₂ O	Ca(OH) ₂	Mn(OH) ₂	MnO ₂	Pb ₃ (PO ₄) ₃ Cl	SiO ₂
50	-9.95	-7.77	-18.88	3.34	-10.69	-5.92	-8.74	11.88	0.30
125	-10.41	-7.99	-19.95	3.87	-11.15	-6.33	-9.70	10.99	0.37
250	-10.84	-7.70	-20.55	5.27	-11.49	-6.28	-10.09	12.04	0.48
375	-11.25	-7.26	-20.65	7.49	-11.81	-6.29	-10.38	13.85	0.48
500	-11.30	-8.19	-21.01	7.68	-11.83	-6.28	-10.38	12.08	0.52
625	-11.57	-7.96	-21.27	8.28	-12.06	-6.53	-10.83	12.54	0.49
Flux (L)	Rhodochrosite	Schwertmannite	Sepiolite	Siderite	Smithsonite		Strengite		
	MnCO ₃	Fe ₈ O ₃ (OH) ₆ (SO ₄)·nH ₂ O	Mg ₄ Si ₆ O ₁₅ (OH) ₇ ·6H ₂ O	FeCO ₃	ZnCO ₃	MgAl ₂ O ₄	FePO ₄ ·2H ₂ O		
50	-1.03	12.54	-3.58	-3.12	-0.99	-0.96	-1.25	-5.91	-0.31
125	-0.82	7.52	-4.31	-2.92	-0.92	-0.89	-1.04	-6.41	-0.44
250	-0.63	6.73	-4.84	-2.70	-0.81	-0.78	-0.86	-6.51	-0.04
375	-0.58	5.89	-5.67	-2.64	-0.81	-0.78	-0.83	-5.96	0.11
500	-0.58	6.27	-5.65	-2.59	-0.77	-0.74	-0.77	-5.68	0.17
625	-0.79	4.89	-6.27	-2.66	-0.80	-0.77	-0.79	-5.77	0.17

Table 7 (continued). Saturation indices (SIs) of selected mineral phases present in effluents from the meso-scale infiltration rig study using layered 3–8 mm crushed Leca® / peat + 10 wt.% limestone / spruce biochar.

Flux (L)	Tenonite	Thenardite	Thermonatrite	Tsumebite	Vivianite	Zincite	Zincosite	Zn(OH) ₂		
	CuO	Na ₂ SO ₄	Na ₂ CO ₃ ·H ₂ O	Pb ₂ Cu(PO ₄) ₂ (SO ₄)(OH)	Fe ₃ (PO ₄) ₂ ·8H ₂ O	ZnO	ZnSO ₄	Zn(OH) ₂	Zn(OH) _{2(am)}	
50	0.00	-9.96	-12.31	-0.73	-7.19	-1.70	-13.15	-2.56	-2.84	
125	-0.13	-10.52	-12.73	-1.37	-7.33	-2.11	-13.08	-2.97	-3.25	
250	0.07	-10.79	-13.22	-0.95	-6.02	-2.07	-12.68	-2.94	-3.21	
375	-0.51	-10.97	-13.59	-0.86	-5.43	-2.10	-12.45	-2.96	-3.24	
500	-0.59	-10.94	-13.61	-1.60	-5.23	-2.03	-12.35	-2.89	-3.17	
625	-0.80	-11.00	-13.82	-1.74	-5.13	-2.08	-12.21	-2.95	-3.22	
Flux (L)	Hoppeite									
	β-Zn(OH) ₂	ε-Zn(OH) ₂	γ-Zn(OH) ₂	Zn ₂ (OH) ₂ SO ₄	Zn ₂ (OH) ₃ Cl	Zn ₃ (PO ₄) ₂ ·4H ₂ O	Zn ₃ O(SO ₄) ₂	Zn ₄ (OH) ₆ SO ₄	Simonkolleite	
	-2.12	-1.90	-2.10	-7.08	-6.62	-1.43	-27.71	-8.70	Zn ₅ (OH) ₈ Cl ₂	
	-2.53	-2.31	-2.51	-7.42	-7.33	-1.56	-27.98	-9.86	-11.73	
	-2.49	-2.27	-2.47	-6.98	-7.02	-0.36	-27.14	-9.35	-13.56	
	-2.52	-2.30	-2.50	-6.79	-7.07	0.14	-26.72	-9.21	-12.90	
	-2.45	-2.23	-2.43	-6.61	-7.05	0.38	-26.45	-8.90	-13.01	
625	-2.50	-2.28	-2.48	-6.53	-7.01	0.61	-26.22	-8.93	-12.92	
									-12.88	

Table 7 (continued). Saturation indices (SIs) of selected mineral phases present in effluents from the meso-scale infiltration rig study using layered 3–8 mm crushed Leca® / peat + 10 wt.% limestone / spruce biochar.

Flux (L)	ZnCl ₂	ZnCO ₃ ·H ₂ O	Zn metal	Zincite	ZnSO ₄ ·H ₂ O
			Zn ⁰	ZnO	
50	-18.82	-0.99	-39.51	-1.55	-8.58
125	-19.02	-0.78	-39.38	-1.96	-8.51
250	-18.51	-0.60	-38.90	-1.92	-8.11
375	-18.52	-0.57	-38.65	-1.95	-7.89
500	-18.70	-0.51	-38.56	-1.88	-7.78
625	-18.43	-0.53	-38.42	-1.94	-7.64